



Miller, Hollie (2024) *Targeted protein degradation of the Y220C-p53 mutant as a potential anti-cancer strategy*. MRes thesis.

<https://theses.gla.ac.uk/84041/>

Copyright and moral rights for this work are retained by the author

A copy can be downloaded for personal non-commercial research or study, without prior permission or charge

This work cannot be reproduced or quoted extensively from without first obtaining permission from the author

The content must not be changed in any way or sold commercially in any format or medium without the formal permission of the author

When referring to this work, full bibliographic details including the author, title, awarding institution and date of the thesis must be given

Enlighten: Theses

<https://theses.gla.ac.uk/>
research-enlighten@glasgow.ac.uk



University
of Glasgow

**Targeted protein degradation of the Y220C-p53 mutant as a
potential anti-cancer strategy**

2023

Hollie Miller

Dr David France and Dr Danny Huang

Declaration of Originality



Declaration of Originality Form

This form **must** be completed and signed and submitted with all assignments.

Please complete the information below (using BLOCK CAPITALS).

Name	HOLLIE MILLER
Student Number	
Course Name	MRES CHEMISTRY
Assignment Number/Name	MRES THESIS

An extract from the University's Statement on Plagiarism is provided overleaf. Please read carefully THEN read and sign the declaration below.

I confirm that this assignment is my own work and that I have:	
Read and understood the guidance on plagiarism in the Undergraduate Handbook, including the University of Glasgow Statement on Plagiarism	<input checked="" type="checkbox"/>
Clearly referenced, in both the text and the bibliography or references, all sources used in the work	<input checked="" type="checkbox"/>
Fully referenced (including page numbers) and used inverted commas for all text quoted from books, journals, web etc. (Please check with the Department which referencing style is to be used)	<input checked="" type="checkbox"/>
Provided the sources for all tables, figures, data etc. that are not my own work	<input checked="" type="checkbox"/>
Not made use of the work of any other student(s) past or present without acknowledgement. This includes any of my own work, that has been previously, or concurrently, submitted for assessment, either at this or any other educational institution, including school (see overleaf at 32.2)	<input checked="" type="checkbox"/>
Not sought or used the services of any professional agencies to produce this work	<input checked="" type="checkbox"/>
In addition, I understand that any false claim in respect of this work will result in disciplinary action in accordance with University regulations	<input checked="" type="checkbox"/>

DECLARATION:
I am aware of and understand the University's policy on plagiarism and I certify that this assignment is my own work, except where indicated by referencing, and that I have followed the good academic practices noted above
Signed..... 15/9/23

The University of Glasgow Plagiarism Statement

The following is an extract from the University of Glasgow Plagiarism Statement. The full statement can be found in the University Calendar at

32.1 The University's degrees and other academic awards are given in recognition of a student's **personal achievement**. All work submitted by students for assessment is accepted on the understanding that it is the student's own effort.

32.2 Plagiarism is defined as the submission or presentation of work, in any form, which is not one's own, without **acknowledgement of the sources**. Plagiarism includes inappropriate collaboration with others. Special cases of plagiarism can arise from a student using his or her own previous work (termed auto-plagiarism or self-plagiarism). Auto-plagiarism includes using work that has already been submitted for assessment at this University or for any other academic award.

32.3 The incorporation of material without formal and proper acknowledgement (even with no deliberate intent to cheat) can constitute plagiarism.

Work may be considered to be plagiarised if it consists of:

- a direct quotation;
- a close paraphrase;
- an unacknowledged summary of a source;
- direct copying or transcription.

With regard to essays, reports and dissertations, the rule is: if information **or ideas** are obtained from any source, that source must be acknowledged according to the appropriate convention in that discipline; and **any direct quotation must be placed in quotation marks** and the source cited immediately. Any failure to acknowledge adequately or to cite properly other sources in submitted work is plagiarism. Under examination conditions, material learnt by rote or close paraphrase will be expected to follow the usual rules of reference citation otherwise it will be considered as plagiarism. Departments should provide guidance on other appropriate use of references in examination conditions.

32.4 Plagiarism is considered to be an act of fraudulence and an offence against University discipline. Alleged plagiarism, at whatever stage of a student's studies, whether before or after graduation, will be investigated and dealt with appropriately by the University.

32.5 The University reserves the right to use plagiarism detection systems, which may be externally based, in the interests of improving academic standards when assessing student work.

If you are still unsure or unclear about what plagiarism is or need advice on how to avoid it,

SEEK HELP NOW!

You can contact any one of the following for assistance:

**Lecturer
Course Leader
Dissertation Supervisor
Adviser of Studies
Student Learning Service**

Abstract

Targeted protein degradation and Proteolysis Targeting Chimeras (PROTACs) in particular, have become an exciting new field in the drug discovery world, with the potential to target previously seen as 'undruggable' proteins. With many PROTACs now reaching the clinic, it is clear that these new modalities have the potential to become therapeutically successful and to overcome problems previously observed with traditional small molecule drugs. One of the most frequently mutated proteins in human cancers, p53 has been a particularly challenging drug target for many years. The work presented in this thesis provides a strategy in which to target and degrade the common Y220C p53 mutant by utilising the PROTAC degradation mechanism.

In particular, PROTAC **2** was found to degrade the Y220C p53 mutant at a low micromolar concentration and hence provides insight into the potential these PROTACs hold for the future as potent degraders of target proteins.

Acknowledgements

I would like to thank Dr David France for giving me the opportunity to work on this research project and for all of his help, expertise and guidance throughout my MRes. I would also like to thank Dr Danny Huang and Dr Feroj Syed of the CRUK-Beatson Institute for allowing me into the lab to observe the biological testing of the compounds and for being very welcoming and encouraging. I would also like to say a special thanks to the France group for being supportive and helpful throughout my time in the group. Finally, I would like to thank the Clark and Prunet groups for making my time in the Henderson Lab so enjoyable.

Table of Contents

Declaration of Originality	2
Abstract	4
Acknowledgements	5
List of Abbreviations	8
Introduction	9
Cancer	9
p53 and the Y220C mutation	10
Known binders of Y220C mutated p53	12
Ubiquitin-proteasome system (UPS)	14
Targeted Protein Degradation	15
PROTACs	16
PROTAC design	18
E3 ligase ligands	18
CRBN ligands	18
Linkers	19
PROTACs bioavailability	19
PROTACs in clinic	20
Drawbacks of PROTACs	21
Project Aims	22
Synthetic Plans	23
Synthesis of PROTAC 1	23
Synthesis of PK9328 warhead for PROTAC 2	24
Synthesis of PROTAC 2	25
Results and Discussion	26
PROTAC 1 and PROTAC 2	26
Physicochemical Properties of PROTAC 1	29
NMR Assignments of PROTAC 1	30
Physicochemical Properties of PROTAC 2	32
NMR Assignments for PROTAC 2	32
PK9328 warhead	35
NMR Assignments for PK9328 warhead	37
Biological testing of compounds	39

Conclusions and Future Work	40
Experimental	41
Chemistry Experimental	41
General Procedures	41
Preparation of compounds	42
Cell Biology Materials and Methods	52
References	53

List of Abbreviations

Abbreviations and acronyms used in this thesis are in agreement with the standard list of abbreviations and acronyms published by The Journal of Organic Chemistry. Non-standard abbreviations and acronyms used in this thesis are listed here.

AR	androgen receptor
BET	bromodomain and extra-terminal domain
BRD9	bromodomain containing 9
BRET	bioluminescent resonance energy transfer
cLogP	calculated partition coefficient
CRBN	cereblon
CRISPR	clustered regularly interspaced short palindromic repeats
Da	dalton
DegS	degradation score
DMF	<i>N,N</i> -dimethylformamide
FBS	fetal bovine serum
HBA	hydrogen bond acceptor
HBD	hydrogen bond donor
ITC	isothermal titration calorimetry
K_D	dissociation constant
LCMS	liquid chromatography–mass spectrometry
logP	partition coefficient
MDM2	mouse double minute-2
MES-SDS	2-(<i>N</i> -morpholino) ethanesulfonic acid-SDS
MOA	mechanism of action
PEG	polyethylene glycol
POI	protein of interest
PROTAC	proteolysis-targeting chimera
SDS	sodium dodecyl sulfate
SDS–PAGE	sodium dodecyl sulfate–polyacrylamide gel electrophoresis
S_N2	substitution nucleophilic bimolecular
TPD	targeted protein degradation
tPSA	topological polar surface area
t_R	retention time
Ub	ubiquitin
UPS	ubiquitin–proteasome system
VHL	von Hippel–Lindau

Introduction

Cancer

According to the World Health Organisation (WHO), in 2020, one of the worldwide leading causes of death was cancer, accounting for around 10 million deaths, with breast, lung and colorectum cancers being the three most common cancer types.¹

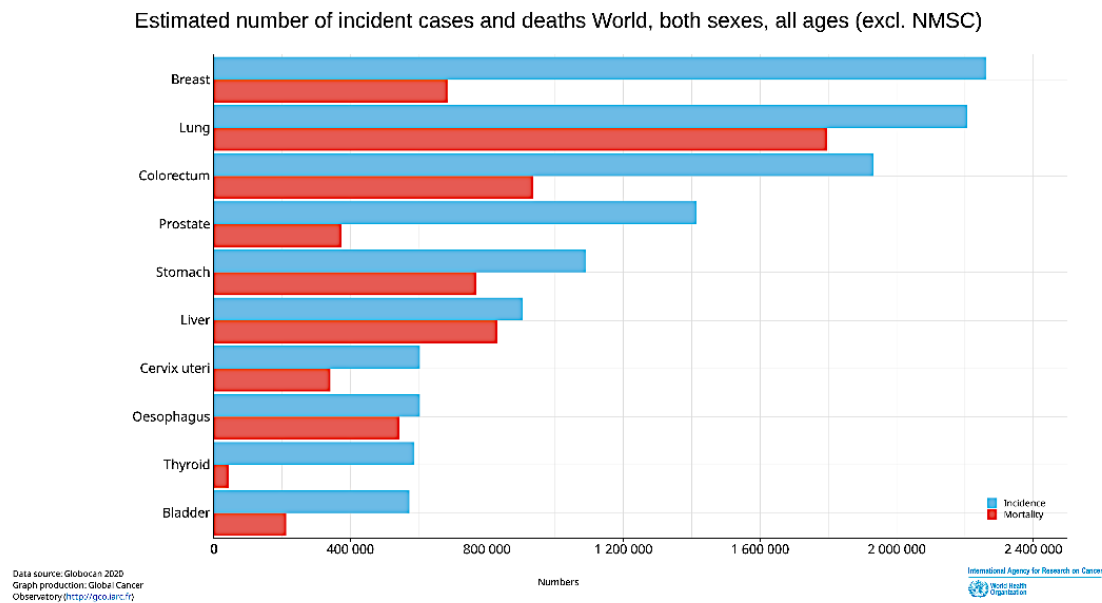


Figure 1: Most common cancer types and corresponding deaths worldwide in 2020 of both sexes and all ages. With incidence shown in blue and mortality in red. Figure sourced from Global Cancer Observatory.²

The overall incidence and mortality of cancer is expected to grow worldwide,³ with the number of new cases expected to rise by approximately 50% by 2040.² This is due to the differences in distribution and prevalence of the major risk factors of cancer and population growth and ageing.⁴ Some of the major risk factors of cancer include smoking, alcohol, diet and infection which vary by country and region.³

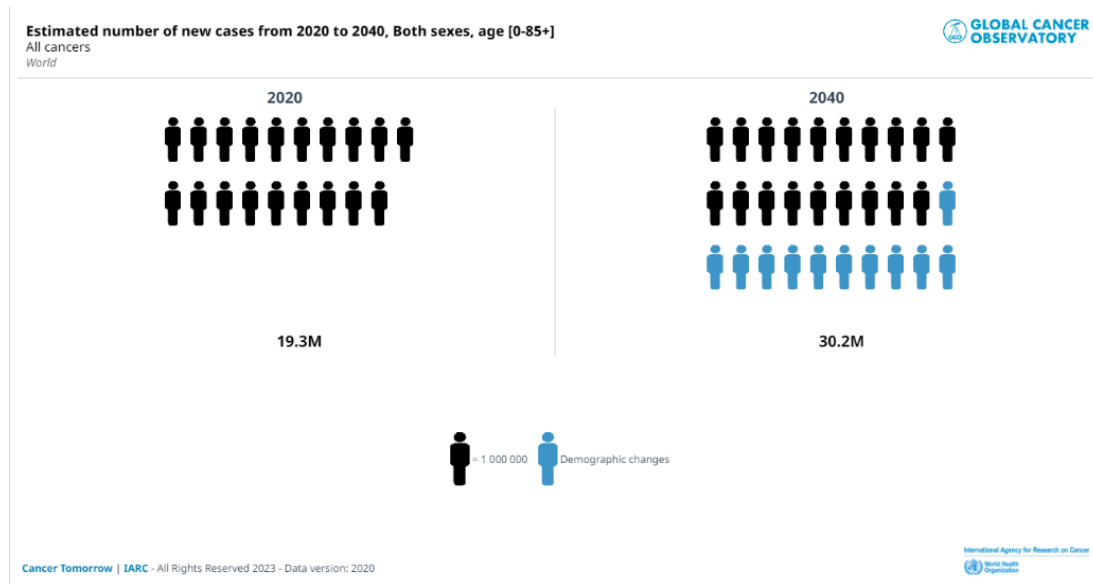


Figure 2: Number of new cancer cases estimated by 2040, including all ages and both sexes. With the black figure representing 1,000,000 new cases and the blue figure representing demographic changes. Figure sourced from Global Cancer Observatory.²

p53 and the Y220C mutation

p53 is a transcription factor which functions as a tumour suppressor through regulating the expression of genes important for cell apoptosis, DNA repair, cell cycle arrest, cellular growth, cellular metabolism and the immune response when exposed to DNA damage or stress stimuli.⁵ In normal conditions, p53 has a half-life of around 5 to 30 minutes.⁶ After this point, it is targeted for ubiquitination and subsequent degradation by the E3 ligase mouse double minute-2 (MDM2) which maintains p53 at low concentrations.⁷ This process is regulated by an autoregulatory negative feedback loop.⁸

In response to stress stimuli or oncogene activation, this degradation process by MDM2 is inhibited, which allows p53 levels to rise and also leads to increased stabilisation of p53, resulting in increased transcription of the genes responsible for damage response mechanisms such as cell cycle arrest and apoptosis (Figure 3).⁶

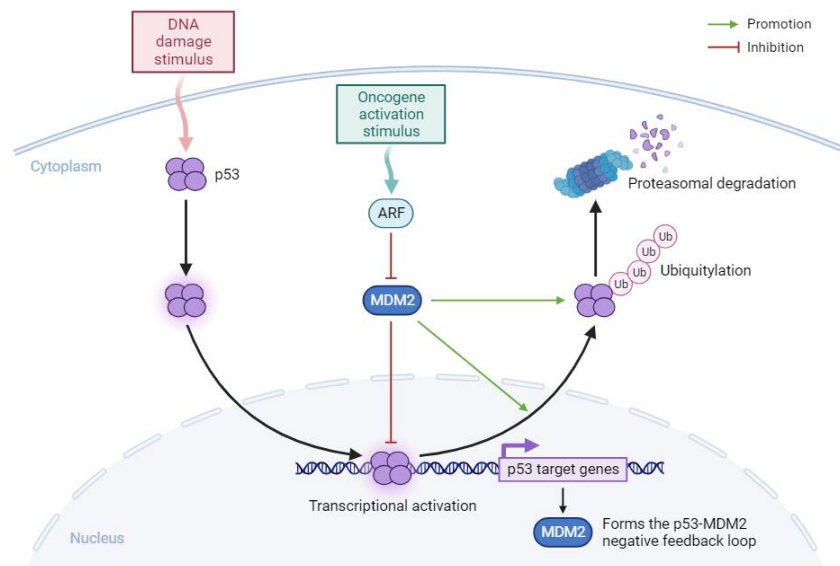


Figure 3: p53 regulation pathway showing the regulation of p53 levels by the E3 ligase MDM2 and the alterations to this pathway during DNA damage or oncogene activation.⁶³

p53 is mutated in around 50% of all cancers, making it a very important target for drug discovery and development.⁹ The p53 protein consists of an N-terminal transactivation domain, a proline-rich domain, a DNA-binding domain (the largest segment) which is also linked to a tetramerisation domain, and a C-terminal regulatory domain.¹⁰ Most p53 mutations are missense mutations, which occur in the DNA-binding domain of p53.¹¹ There is also evidence to suggest that mutated p53 can exhibit gain-of-function properties or increased oncogenic effects, whereby it can promote metastasis and drug resistance,¹² so mutation of p53 is more detrimental than simply the loss of a wild-type p53 protein.¹³ Heterotetramers can form between mutated p53 and wild-type p53, reducing the effectiveness of the wild-type p53 to bind with its targets.¹⁴ This is thought to cause a dominant negative effect on the wild-type activity of p53, counteracting the tumour suppression role of p53. Heterotetramer formation is favoured due to the higher concentration of mutant p53 present compared to the wild-type, so it is proposed that removal of the mutant p53 could restore the wild-type tumour suppression activity of p53.¹⁵

The Y220C mutation is the most common mutation to occur out-with the DNA-binding domain of p53, occurring instead on the β -sandwich region of p53.¹⁶ Mutations in this β -sandwich region are reported for around one third of cancer cases. The Y220C mutation forms a solvent-exposed cavity on the end of the β -sandwich region, while still maintaining functionally important wild-type structural properties as the core domain remains intact. This cavity formed by the Y220C mutation is an attractive drug target for the rescue of wild-type behaviour and since the mutation occurs on the β -sandwich region and not on the DNA-binding domain, it is far from the functional area of the protein.¹⁷ In the Y220C mutation, a tyrosine is replaced by a cysteine¹⁸ which destabilises the p53 protein by around 4 kcal/mol, due to the loss of hydrophobic interactions within the region.¹⁷

Known binders of Y220C mutated p53

p53 has been an attractive target for drug development for many years because of its known function as a tumour suppressor.¹⁹ Duffy *et al.* have shown that the tumour suppression activity of p53 can be restored, as several p53 mutations change the conformation of p53 and reversing this conformational change may recover the wild type conformation.²⁰ Hence, there have been efforts made to discover small molecules that will restore the wild-type transcriptional and tumour suppressive activity of p53.¹²

One such molecule that has been shown to restore the p53 wild type activity is the carbazole containing PhiKan083 (Table 1).²¹ PhiKan083 was designed to bind to the specific cavity created by the Y220C mutation of p53 and so by doing this it would bind in a weaker manner to the wild-type protein. PhiKan083 was found to bind to this Y220C induced cavity with a K_d of 125 μ M (Table 1) determined from isothermal titration calorimetry.²¹

The crystal structure of PhiKan083 bound to the Y220C mutant of p53 was solved which allowed key interactions within the binding site to be analysed.²¹ This crystal structure revealed that the main carbazole ring system is mostly buried in the cavity where it sits between two sets of hydrophobic side chains on either side of the cavity, indicating that binding is impacted by hydrophobic packing interactions. The nitrogen of the carbazole ring system is found close to the position of the hydroxyl group from the wild-type tyrosine residue and the ethyl chain of PhiKan083 was shown to anchor

the molecule in the cavity where it is in close proximity with the mutated Cys-220 residue.²¹ The methylmethanamine chain of PhiKan083 is solvent exposed²² and forms a hydrogen bond to a carbonyl of the Asp-228 residue in the hydrophilic section of the cavity.²¹

Another carbazole containing small molecule binder of the p53-Y220C mutant that has been discovered is the PK9328 molecule (Table 1).²² PK9328 is a potent binder of p53-Y220C, with a K_d of 1.7 μM . It has been shown that introducing a five-membered heterocycle, specifically a thiophene, at the C-7 position of the PhiKan083 carbazole system increases its binding affinity to 2.6 μM as it can fill a subsite of the p53-Y220C mutant that was previously unoccupied. Introduction of a methyl group on the C-4 position of the thiophene resulted in the potent PK9328.

Another potent small molecule binder of the p53-Y220C mutant is the aminobenzothiazole JC744, which binds with a K_d of 320 nM (Table 1).²³ JC744 is the most potent binder of p53-Y220C recorded to date and has also been reported to stabilise the p53 protein with a ΔT_m of 2.7 $^\circ\text{C}$ observed.

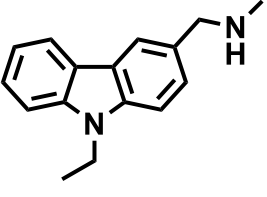
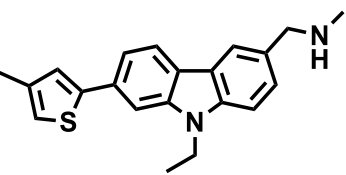
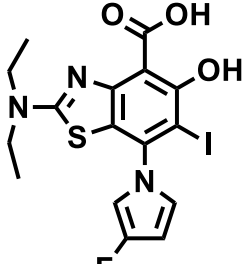
Y220C binder	 PhiKan083	 PK9328	 JC744
K_d	125 μM ²¹	1.7 μM ²²	320 nM ²³
ΔT_m ($^\circ\text{C}$)	2.0 ²¹	3.3 ²²	2.7 ²³

Table 1: Most potent binders of p53 Y220C mutant reported in the literature. Table showing the binding affinities (K_d) and melting temperature changes (ΔT_m) for each binder.

Ubiquitin-proteasome system (UPS)

The process of ubiquitination was awarded the Nobel Prize in Chemistry in 2004.²⁴ Ubiquitination is the post-translational process by which proteins are targeted for degradation by the proteasome through the attachment of ubiquitin.²⁵ Ubiquitin itself, is a small protein which consists of 76 amino acids and it attaches to the target protein through an isopeptide bond with a lysine residue.²⁶ The process of ubiquitination involves the use of E1, E2 and E3 enzymes. The E1 enzyme is responsible for activation of ubiquitin in an ATP-dependent manner, it is then transferred to the E2 enzyme, which is a carrier enzyme for ubiquitin, where it is then transferred by the ubiquitin-protein ligase E3 enzyme to the target protein (Figure 4).²⁵

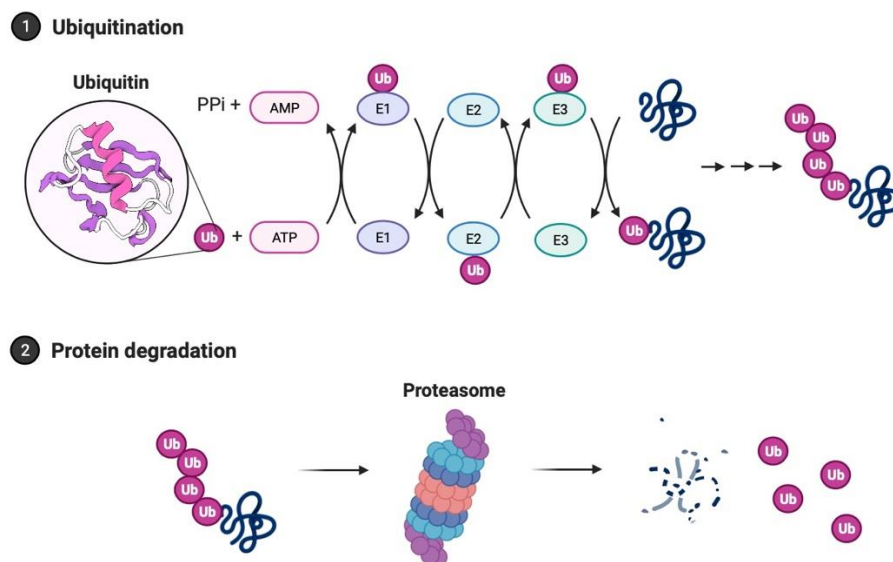


Figure 4: Illustration of the ubiquitin-proteasome system.^{25,63}

The ubiquitin-proteasome system (UPS) is a vital system for maintaining protein homeostasis within cells. Due to the vital role of the UPS, impairment can result in cancers, neurodegenerative diseases and also viral disease.²⁷

Targeted Protein Degradation

Small molecule drugs have been the primary focus of drug development for many years. However, these small molecule drugs require a defined active site and so cannot be used against every drug target.²⁸ These small molecule drugs usually function through what is known as occupancy-driven pharmacology, which relies on a high dose of the drug to be administered in order to maintain a high occupancy of the target,²⁸ due to reversible binding.²⁹ This method of pharmacology may result in side effects, due to the off target binding that occurs at these high drug concentrations.²⁸

Targeted protein degradation (TPD) is a relatively new field of drug discovery, which often utilises the UPS to artificially recruit E3 ligase enzymes within cells to degrade unwanted proteins.³⁰ Using TPD is considered as a way to target previously reported “undruggable” protein targets, such as transcription factors.³¹ Transcription factors usually contain complex and disordered regions within their quaternary structure or have a large, flat surface area to aid in the formation of protein-protein interactions.³² Another advantage of TPD, is that it can be used in substoichiometric doses compared to traditional small-molecule inhibitors.³¹

PROTACs

Proteolysis-targeting chimeric molecules (PROTACs) are heterobifunctional molecules that were first reported by Crews *et al.* in 2001.³³ They consist of a ligand which is specific for the protein of interest (POI), a ligand which is specific for an E3 ligase enzyme and a linker which connects the two ligands (Figure 5).³⁴

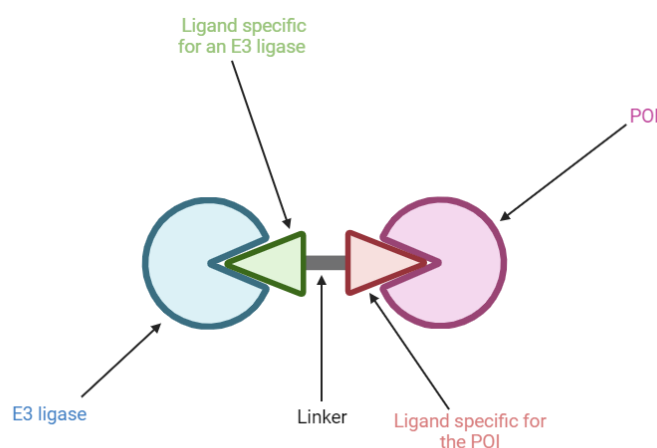


Figure 5: Illustration of a proteolysis targeting chimera (PROTAC), showing the POI, the E3 ligase, the two ligands specific for both the POI and the E3 ligase and the linker used to attach both ligands.⁶³

The PROTAC molecule is able to bind simultaneously to both the E3 ligase and the POI, which then folds in on itself, allowing the POI to be in close proximity to the E3 ligase. This facilitates protein-protein interactions between the POI and the E3 ligase and a stable ternary complex is formed.³⁵ After formation of the ternary complex, the E3 ligase will ubiquitinate the POI leading to polyubiquitination. The POI is then recognised and degraded by the proteasome. The PROTAC is regenerated and is available for recruitment of another POI molecule meaning the PROTAC is catalytic in nature (Figure 6).³⁶

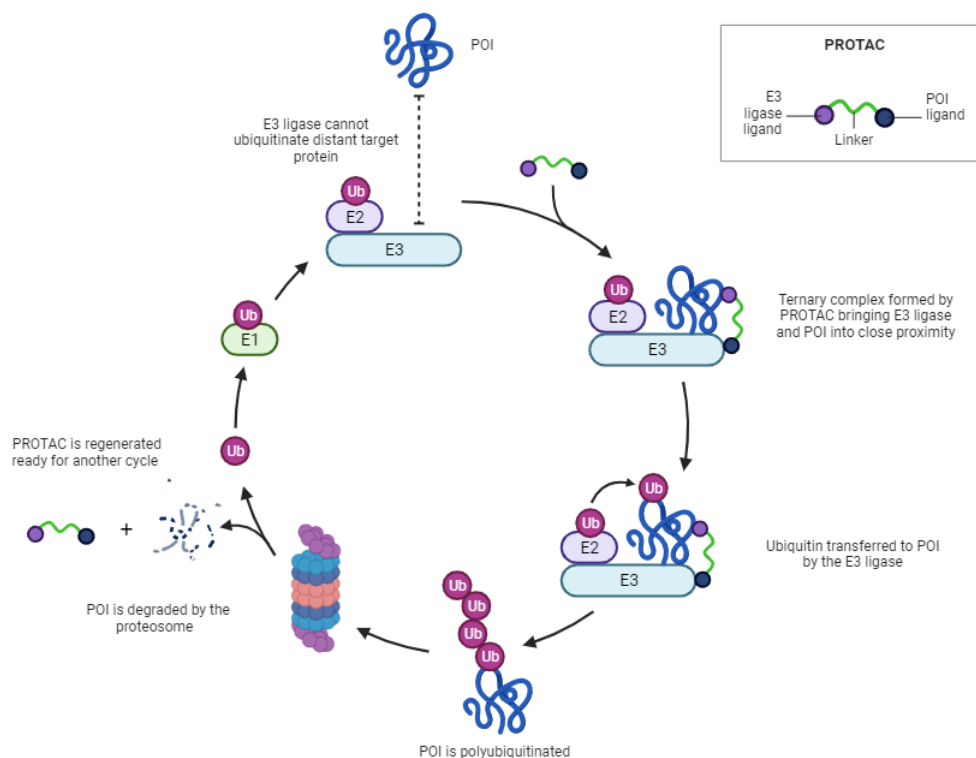


Figure 6: PROTAC mechanism of action.^{35, 36, 63}

This mechanism of action (MOA) of PROTAC molecules is known as an event-driven MOA, which is an alternative to the traditional occupancy-driven MOA employed by small-molecule drugs.³⁷ This event-driven MOA and catalytic nature of the PROTAC allows for lower drug doses to be administered, as there is no longer a requirement for a high occupancy of the target protein to achieve the desired effect of protein degradation, reducing the possibility of off-target binding and side effects.³⁸

PROTACs also present a way to target proteins previously thought to be “undruggable”, as they do not rely on the target possessing an active site or any enzymatic activity as they can bind anywhere on a substrate.³⁵ PROTACs also present a way to potentially overcome drug resistance, which is commonly seen with small-molecule drugs as they can degrade proteins that have scaffolding roles, preventing downstream signalling from occurring.³⁵ Mutation is also a common form of drug resistance seen with small-molecule drugs, especially in cancer. PROTACs could overcome this as they only rely on the formation of a transient association with the

target protein and, therefore, a mutation of the protein may not affect the ability of the PROTAC to degrade the mutant protein.³⁹

PROTAC design

It is important to carefully consider the components of the PROTAC in order to achieve a potent degrader. The correct E3 ligase, linker type and linker length must be chosen in order to achieve potent degradation of the POI.

E3 ligase ligands

Despite the fact that the human genome contains more than 600 E3 ligases, only a small selection of these have been utilised in the design of PROTACs.⁴⁰ The peptide-like nature of known E3 ligase ligands limits the choice of the E3 ligase ligand for use in PROTACs due to their lack in stability, permeability and synthetic accessibility, therefore, it remains a challenge to discover E3 ligase ligands with better drug-like characteristics.⁴¹ The two most commonly used E3 ligases targeted by PROTACs are cereblon (CRBN) and von Hippel-Lindau (VHL).⁴⁰ For the purpose of this project only the ligands for the CRBN E3 ligase will be discussed.

CRBN ligands

The drug thalidomide was discovered in 1957 and was used to treat insomnia, however, it was later found to have devastating teratogenic effects and was soon taken off the market.⁴² It was later found that thalidomide and its derivatives pomalidomide and lenalidomide (Figure 7) were capable of binding to the E3 ligase CRBN.⁴³ There has been successful use of CRBN as an E3 ligase in PROTACs to target more than 30 different proteins so far, including proteins for immune disorders and various cancers.⁴⁰

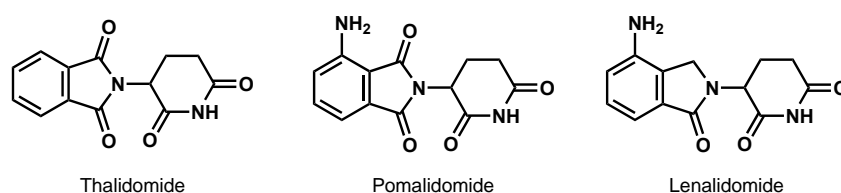


Figure 7: Structures of thalidomide and its derivatives pomalidomide and lenalidomide.⁴³

Linkers

The choice of linker used within a PROTAC plays a critical role in both its resulting biological and physiochemical features.⁴⁴ The length of the linker used is important to consider. If the linker is too long, the PROTAC molecular weight will increase, decreasing cell permeability.⁴⁴ Increasing linker length also destabilises ternary complex formation, due to increasing distance between the POI and E3 ligase. Hence, this would decrease the association constant of binding between the two. The use of polyethylene glycol (PEG) linkers can increase water solubility of the PROTAC, due to their hydrophilic nature and also adds flexibility. Increasing the rigidity of a linker can also have beneficial properties, such as the potential ability to lock the PROTAC in its biologically active conformation. Use of a piperazine within the linker increases rigidity, as well as improving water solubility due to its hydrophilic nature.⁴⁴

PROTACs bioavailability

In 1997, Lipinski developed a guide known as the 'rule of 5' (Table 2) to assess the oral bioavailability of drug candidates, in which a number of physiochemical properties are assessed to determine if a compound would be orally bioavailable or not.⁴⁵

Hydrogen bond donors	≤5
Molecular Weight (Da)	≤500
Log P	≤5
Hydrogen bond acceptors	≤10

Table 2: Lipinski's 'Rule of 5'.⁴⁵

However, Lipinski's guidelines will usually only apply to small molecule drugs, since they require the drug candidate to have a molecular weight of less than 500 Daltons (Da). Hence, the Lipinski guidelines cannot be applied to PROTACs, since the majority of PROTACs have a molecular weight exceeding that of 500 Da.⁴⁵

In 2019, Maple *et al.* re-evaluated Lipinski's 'rule of 5' to establish a new set of parameters for heterobifunctional degraders.⁴⁶ This was done by creating a degrader score (DegS) for 422 degraders. The average value for a range of physiochemical properties of the highest scoring degraders (DegS ≥ 4), degraders with the best ability to induce degradation of their POI, were determined and can be seen in Table 3.

Molecular Weight (Da)	985
cLogP	5.36
Hydrogen Bond Donors	4.13
Hydrogen Bond Acceptors	13.3
Number of rotatable bonds	24.6
tPSA (Å ²)	208

Table 3: Optimal physicochemical parameters for a heterobifunctional degrader as determined by Maple et al.⁴⁶

PROTACs in clinic

Arvinas Therapeutics, launched the first PROTAC to enter stage one clinical trials in 2019. The PROTAC ARV-110 (Figure 8), was developed by Arvinas Therapeutics to target the androgen receptor (AR) for degradation.⁴⁷ The AR is known as a nuclear hormone receptor, which can be activated by the testosterone and dihydrotestosterone male sex hormones. The AR plays a vital role in normal prostate development, however, it is also a driving force for the development of metastatic prostate cancer.⁴⁸ Antiandrogen drugs have been developed and have shown good clinical success in patients with metastatic prostate cancer, however, there exists a number of resistance pathways against these drugs, so alternative AR target therapies are required to overcome this resistance battle.⁴⁸ ARV-110 was found to be a safe, orally bioavailable degrader of AR with promising results in the clinic showing 70 – 90% degradation of the AR in one patient.⁴⁷

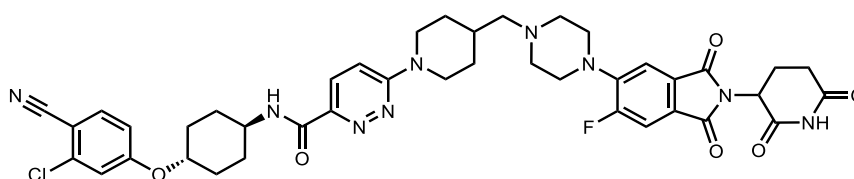


Figure 8: Structure of PROTAC ARV-110, developed by Arvinas Therapeutics.⁴⁹

In 2022, C4 Therapeutics announced the launch of their heterobifunctional degrader, CFT8634 into the clinic.⁵⁰ The CFT8634 (Figure 9) degrader was developed for the degradation of BRD9, a bromodomain protein. BRD9 plays a vital role in the rare synovial cancer, where it acts as a potential scaffolding protein.⁴⁷ BRD9 has been viewed as an “undruggable” target, as screening campaigns have failed to identify an inhibitor of BRD9.⁵⁰ However, CFT8634 has shown to be a potent degrader of BRD9.⁵⁰

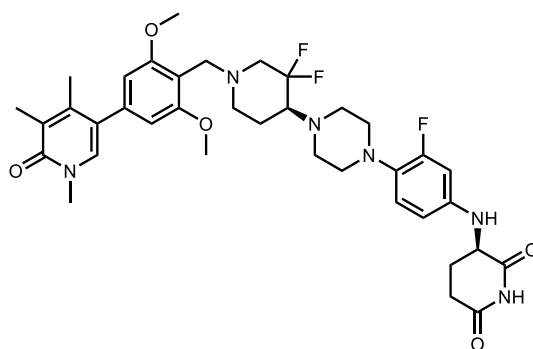


Figure 9: Structure of PROTAC CFT8634 developed by C4 Therapeutics.⁵¹

Drawbacks of PROTACs

Despite their many advantages, PROTACs have limitations. Only a limited number of E3 ligases have been utilised in PROTACs, despite the large number available in the human genome and already drug resistance has been observed in tumours against the CRBN and VHL targeting ligands.⁵² Therefore, it is necessary to explore other E3 ligases which can be targeted by PROTACs in the future.

Although PROTACs have the potential to overcome resistance, in certain cases resistance to PROTACs might develop.^{53,54} Cancer cells have shown an ability to develop resistance towards other therapies within a few months of treatment and so it is likely that they will also develop resistance mechanisms to PROTACs. Examples of resistance have already been shown towards bromodomain and extraterminal domain (BET) PROTACs, which target the VHL and CRBN E3 ligases. It was determined that resistance towards these PROTACs was formed through E3 ligase machinery alterations.⁵⁴

Project Aims

The overall aim for this project was to design and synthesise two PROTACs capable of inducing the degradation of the Y220C p53 mutant and to synthesise the compound PK9328,²² a potent binder of Y220C p53 mutant (Table 1). The physicochemical properties: molecular weight, cLogP, number of hydrogen bond donors and acceptors, number of rotatable bonds and the topological polar surface area (tPSA) of both PROTACs will then be determined using SwissADME.⁶⁴ The second aim is to subsequently test the synthesised PROTACs and the PK9328 compound for biological activity against the Y220C p53 mutant.

PROTAC **1** was designed and synthesised based on previous work within the group where it displayed biological activity against Y220C p53 mutant. The warhead ligand of PROTAC **1**, which would target the POI, was selected to have the structure of PhiKan083²¹ based on its known ability to bind to the Y220C p53 mutant (Table 1). PROTAC **1** was designed to also contain a triethylene glycol linker and a CRBN E3 ligase recruiting ligand (Figure 10).

PROTAC **1** could be optimised to generate PROTAC **2**, by replacing the warhead ligand PhiKan083²¹ for the PK9328²² ligand (Table 1), which displays a stronger binding affinity towards the Y220C mutated p53 (Figure 10).

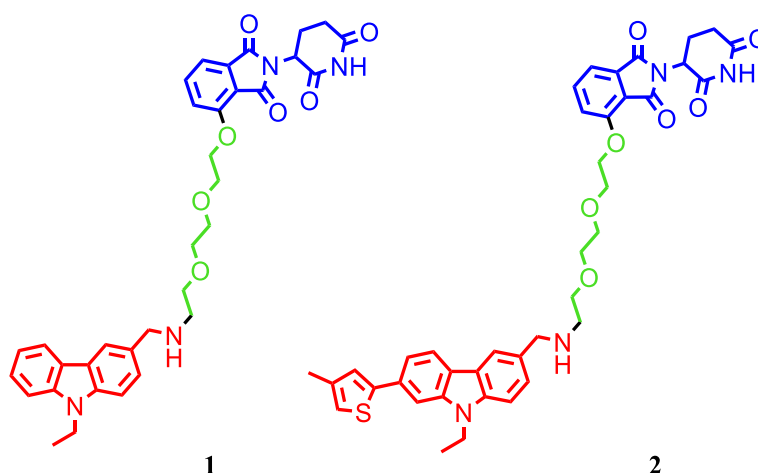
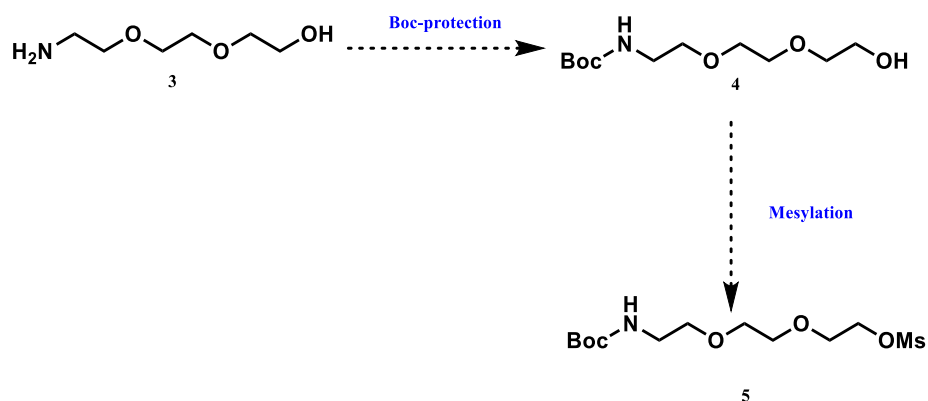


Figure 10: Structures of PROTACs **1** and **2**. Showing the E3 ligase ligand in blue, the POI ligand in red and the linker in green.

Synthetic Plans

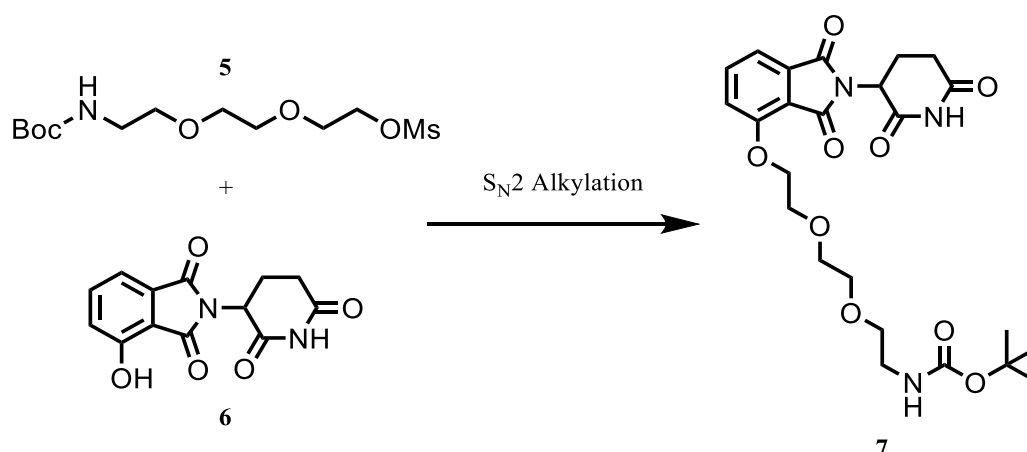
Synthesis of PROTAC 1

The synthetic plan for PROTAC **1** was to initially form mesylated linker **5** through boc-protection of amine **3**, followed by subsequent activation of the alcohol **4** through reaction with mesyl chloride (Scheme 1).



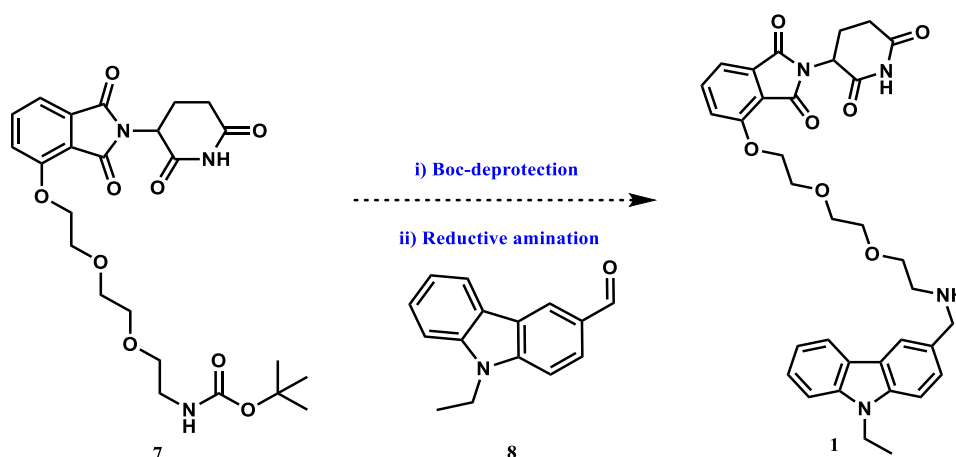
Scheme 1: Formation of the activated mesylate linker 5.

After formation of the mesylated linker **5**, PROTAC **1** could be assembled. Firstly, the mesylate linker **5** would be attached to the 4-hydroxy CRBN ligand **6** through an S_N2 alkylation reaction, affording the fragment **7** (Scheme 2).



Scheme 2: Formation of the fragment 7 by S_N2 alkylation.

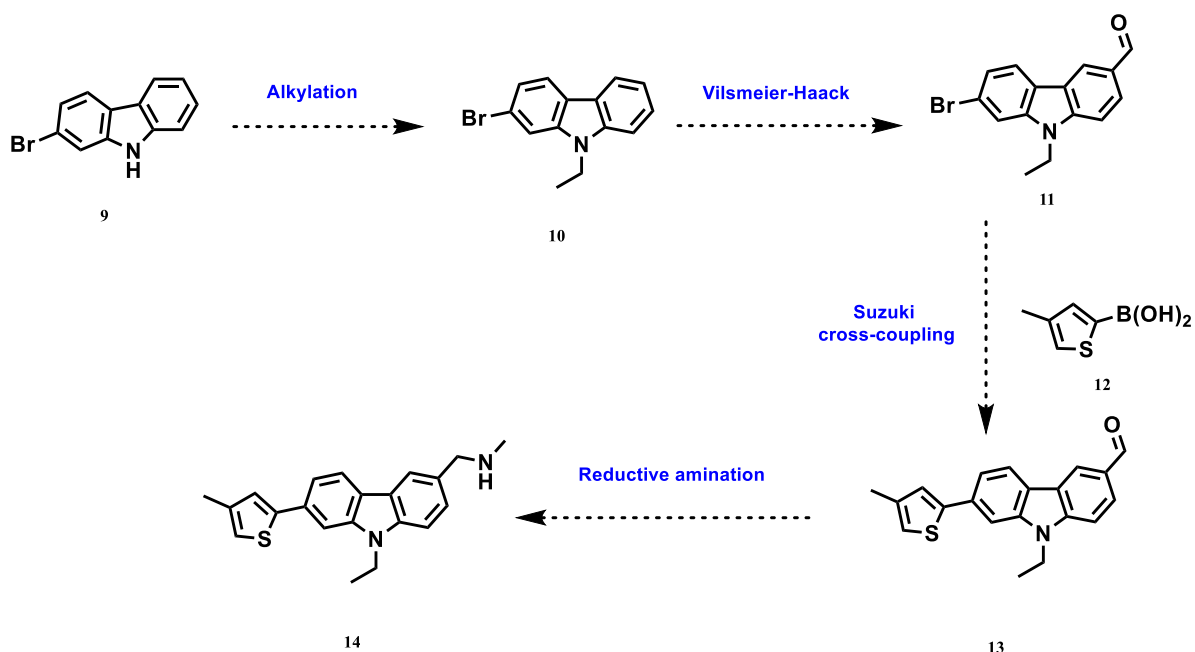
This fragment could then undergo deprotection for removal of the boc-protecting group, followed by subsequent reductive amination with the aldehyde **8**, to yield the desired PROTAC HM-I-37 **1**, ready for subsequent biological testing (Scheme 3).



Scheme 3: PROTAC **1** synthesis from deprotection and reductive amination of fragment **7**.

Synthesis of PK9328 warhead for PROTAC **2**

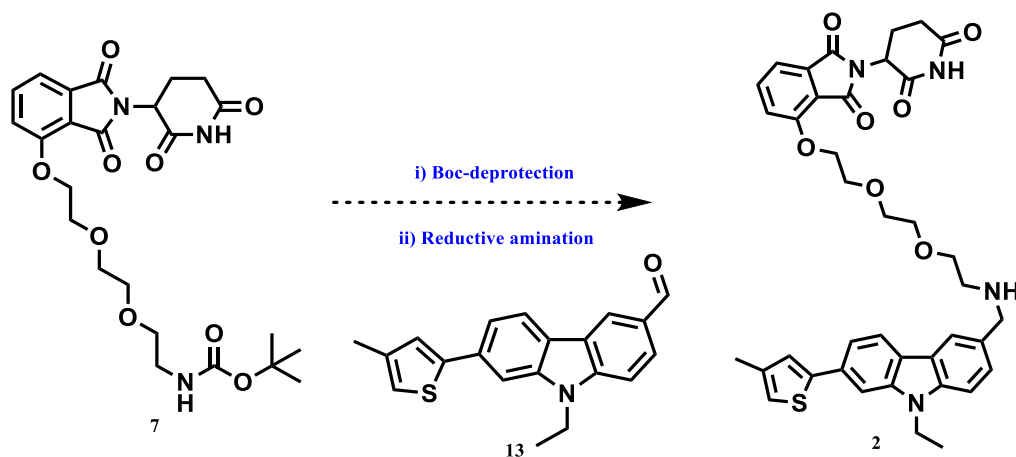
The synthetic plan for synthesis of PROTAC **2** warhead PK9328 **14** (HM-I-34) would begin with alkylation of carbazole **9**. The resulting ethyl carbazole **10** would then be subjected to a Vilsmeier-Haack reaction, giving aldehyde **11**, which would then undergo Suzuki cross-coupling with the boronic acid **12** to produce the methyl thiophene aldehyde **13**. The final step to yield the desired PK9328 warhead **14** is the reductive amination of aldehyde **13** (Scheme 4).



Scheme 4: Synthetic route for PK9328 warhead **14**.

Synthesis of PROTAC 2

The synthetic route towards PROTAC **2** (HM-I-35) was analogous to that of PROTAC **1**, using the mesylate linker **5** and attaching this to the CRBN ligand **6** through S_N2 alkylation (Scheme 2). The resulting fragment **7** would then be subjected to boc-deprotection and subsequent reductive amination with the aldehyde **13** to yield the desired PROTAC **2** (Scheme 5).

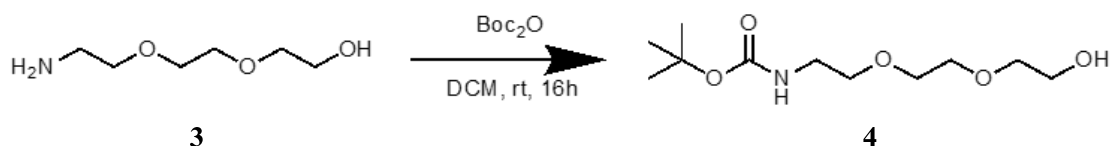


Scheme 5: PROTAC **2** synthesis from deprotection and reductive amination of fragment **7**.

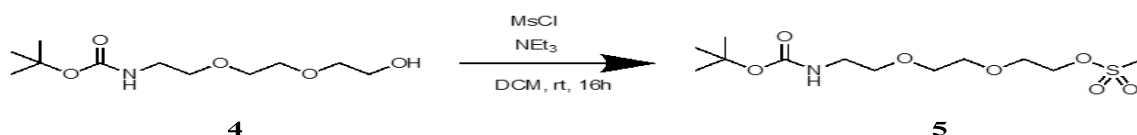
Results and Discussion

PROTAC 1 and PROTAC 2

The synthesis of PROTAC **1** and **2** began with the boc-protection of linker **3** which afforded the protected alcohol **4** in 79% yield (Scheme 6), this then underwent mesylation which was successful producing **5** in quantitative yield (Scheme 7).

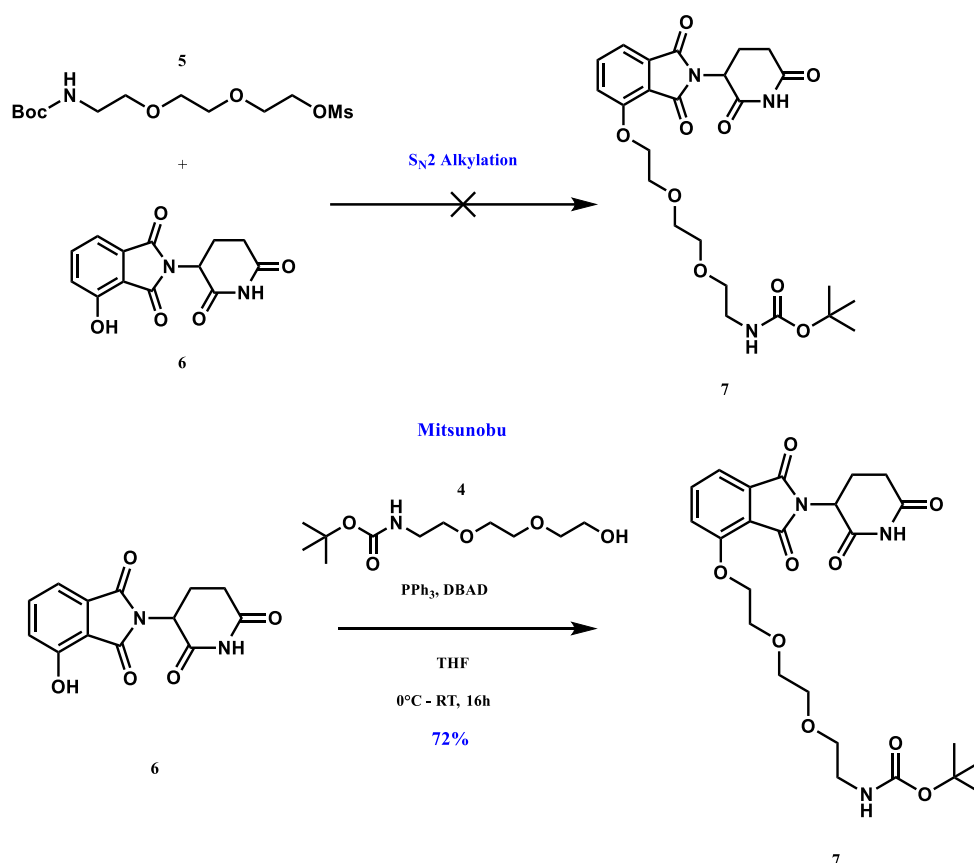


Scheme 6: Synthesis of boc-protected alcohol **4**.



Scheme 7: Synthesis of mesylate linker **5**.

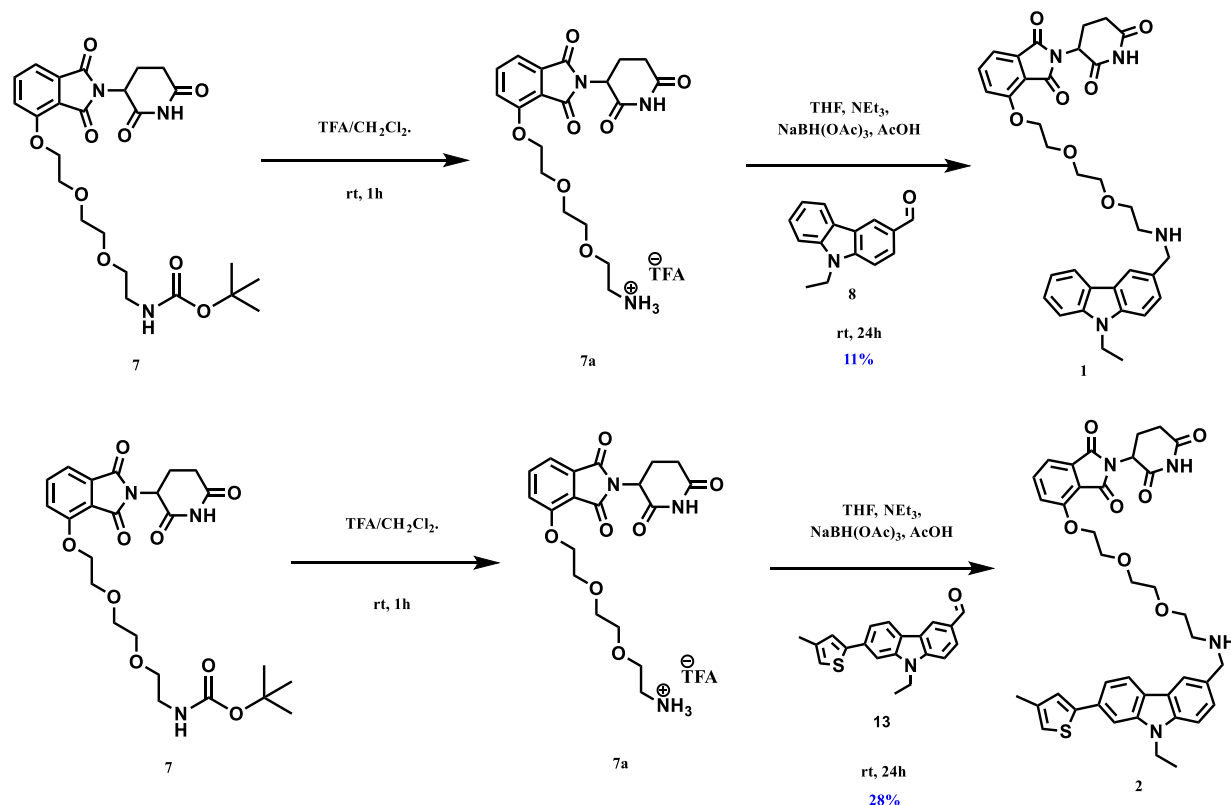
Unfortunately, the S_N2 alkylation of CRBN ligand **6** with mesylate linker **5** was unsuccessful with no product **7** observed for reasons not ascertained, therefore, an alternative route was required. An O-alkylation Mitsunobu reaction was attempted following a similar protocol to literature precedent (Scheme 8).⁵⁵ The Mitsunobu reaction utilised excess CRBN ligand **6**, which was easy to remove by aqueous washing with sodium bicarbonate and the triphenyl phosphine oxide produced was removed via column chromatography. The Mitsunobu reaction proved to be successful in synthesising product **7** from reaction of the CRBN ligand **6** and the alcohol linker **4** to afford **7** in 72% yield (Scheme 8).



Scheme 8: Attempted formation of fragment 7 by S_N2 alkylation and successful synthesis of fragment 7 through Mitsunobu reaction.

The final step in the synthesis of PROTAC **1** and **2** was the deprotection of the Boc-group, followed by the reductive amination with the aldehydes **8** and **13** for PROTAC **1** and **2** respectively (Scheme 9). Boc-deprotection of fragment **7** to the resulting trifluoroacetate salt **7a** (Scheme 9) was monitored to full conversion using TLC and NMR. As the trifluoroacetate salt **7a** was used for the reductive amination reaction with aldehyde **8** and **13**, four equivalents of triethylamine was added to the reaction mixture in order to form the free amine and neutralise any remaining trifluoroacetic acid after concentration. Acetic acid was also added to catalyse the formation of the imine during the reductive amination reaction. Sodium triacetoxyborohydride was selected as the reducing agent for the formation of PROTAC **1** and **2**, as it is a milder reducing agent in comparison to the frequently used sodium borohydride and sodium cyanoborohydride. An advantage of this milder reducing property, is that sodium triacetoxyborohydride is slow to reduce aldehydes and ketones which allows it to be used in a one-pot reductive amination.⁵⁶ (Scheme 9). Analysis by 1H and ^{13}C NMR

confirmed the synthesis of PROTACs **1** (Table 5 and 6) and **2** (Table 8 and 9) affording PROTAC **1** in 11% yield and PROTAC **2** in 28% yield over two steps.



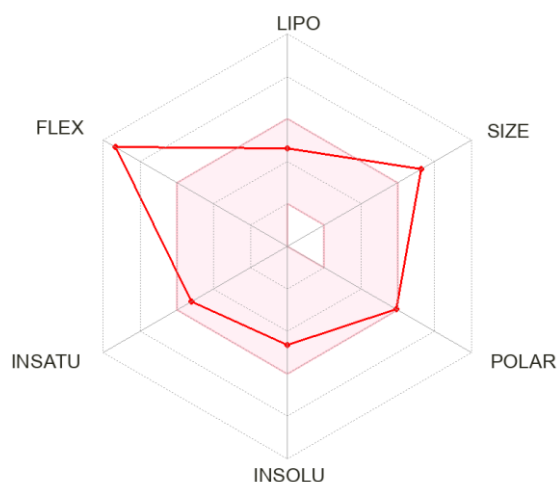
Scheme 9: Formation of PROTAC **1** and **2** through boc-deprotection and subsequent reductive amination.

The physicochemical properties: molecular weight, cLogP, Log S, fraction Csp3, number of rotatable bonds and the topological polar surface area (tPSA) of both PROTACs **1** and **2** were determined using SwissADME.⁶⁴ The results gave insight into the drug likeness of both PROTAC **1** and **2** (Table 4 and 7). The physicochemical properties of both PROTAC **1** and **2** does not conform to the Lipinski guidelines,⁴⁵ as they both have a molecular weight exceeding 500 Da. Using Lipinski's guidelines, this would suggest that PROTAC **1** and **2** would not be orally bioavailable, however, they do fit into the Maple *et al.*⁴⁶ set of guidelines which were developed for heterobifunctional degraders. This suggests that both PROTACs **1** and **2** have the potential to be orally bioavailable.

From the physicochemical properties of both PROTACs **1** and **2**, it can be observed that the introduction of the 4-methyl thiophene onto the carbazole warhead of the

PROTAC, as seen in PROTAC **2**, increases the cLogP value by more than 1 (Table 7). This makes the PROTAC more lipophilic, which is a desirable property as a small increase to the cLogP of a compound has been known to improve the oral bioavailability.⁵⁷ However, the introduction of this thiophene also increases the tPSA (Table 7), due to the increase in polarity and size of the PROTAC. This is thought to decrease the oral bioavailability of the compound, as this can make it harder for the compound to exhibit passive permeability through intestinal membranes.⁵⁷ PROTAC **2** also exhibits an increased number of rotatable bonds (Table 7), which is known to decrease oral bioavailability of a compound, as the compound is more flexible and so can adopt more conformations which involves a greater loss of entropy during the binding to and passage through cellular membranes.

Physiochemical Properties of PROTAC 1



Physiochemical Property	Related Chemical Property	Value
Size	Molecular Weight (Da)	613
Lipophilicity	cLogP	3.07
Insolubility	Log S	- 4.65
Insaturation	Fraction Csp3	0.35
Flexibility	Number of rotatable bonds	14
Polarity	tPSA (Å ²)	128

Table 4: Physiochemical and corresponding chemical properties determined for PROTAC **1** using SwissADME.⁶⁴

NMR Assignments of PROTAC 1

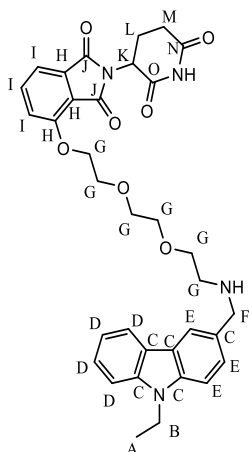


Figure 11: Structure of PROTAC 1 with H and C assignment letters.

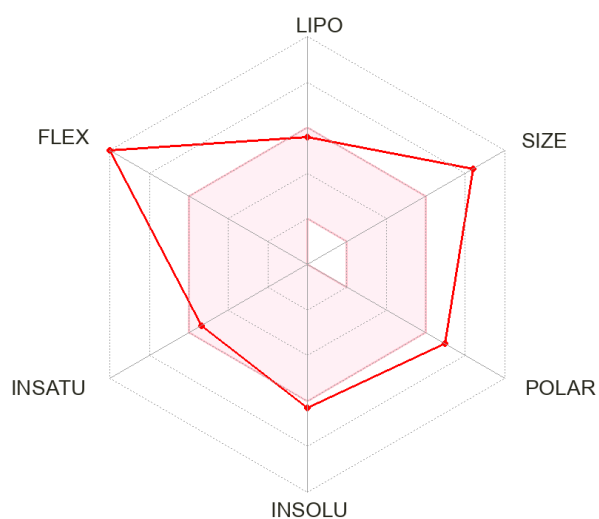
Shift (ppm)	Integration	Multiplet	J-value (Hz)	Assignment
8.09-8.03	2H	m		E
7.54	1H	dd	8.4, 7.3	I
7.48-7.37	4H	m		D
7.34	1H	d	8.4	I
7.20	1H	ddd	8.4, 7.1, 1.0	E
7.12	1H	d	8.4	I
4.90	1H	dd	12.0, 5.2	K
4.34	2H	q	7.2	B
4.25	2H	t	4.5	G
3.99	2H	s		F
3.92-3.89	2H	t	4.8	G
3.79-3.75	2H	m		G
3.67-3.61	2H	m		G
2.89	2H	t	5.4	G
2.86-2.60	3H	m		L and M
2.10-2.02	1H	m		M
1.41	3H	t	7.2	A

Table 5: ^1H NMR assignments for PROTAC 1. Assignment letters can be seen in figure 11.

Shift (ppm)	HSQC	Assignment
171.0	Q	N
168.2	Q	O
167.1	Q	J
165.7	Q	J
156.5	Q	H
140.3	Q	H
139.4	Q	H
136.5	Ar-CH	I
133.8	Q	C
130.4	Q	C
126.5	Ar-CH	E
125.7	Ar-CH	D
123.1	Q	C
122.9	Q	C
120.6	Ar-CH	E
120.4	Ar-CH	E
119.6	Ar-CH	I
118.9	Ar-CH	E
117.4	Q	C
116.2	Ar-CH	D
108.6	Ar-CH	D
108.4	Ar-CH	D
71.2	CH ₂	G
70.5	CH	G
69.5	CH ₂	G
69.4	CH ₂	G
54.3	CH ₂	F
49.2	CH	K
48.7	CH ₂	G
37.7	CH ₂	B
31.5	CH ₂	L
31.5	CH	M
22.8	CH	M
14.0	CH ₃	A

Table 6: ¹³C NMR assignments for PROTAC 1. HSQC was used to determine C environment. Where Q is quaternary carbon and Ar-CH is aromatic CH. Assignment letters can be seen in figure 11

Physiochemical Properties of PROTAC 2



Physiochemical Property	Related Chemical Property	Value
Size	Molecular Weight (Da)	709
Lipophilicity	cLogP	4.64
Insolubility	Log S	-6.30
Insaturation	Fraction Csp3	0.33
Flexibility	Number of rotatable bonds	15
Polar	tPSA (Å ²)	156

Table 7: Physiochemical and corresponding chemical properties determined for PROTAC 2 using SwissADME.⁶⁴

NMR Assignments for PROTAC 2

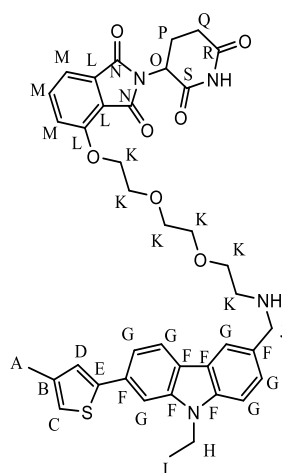


Figure 12: Structure of PROTAC 2 with H and C assignment letters.

Shift (ppm)	Integration	Multiplet	J-value (Hz)	Assignment
8.06-7.99	2H	m		G
7.55-7.50	2H	m		M
7.44	2H	ddd	9.5, 6.2, 1.4	G
7.39	1H	d	7.0	M
7.32	1H	d	8.3	G
7.23-7.22	1H	d	1.2	C/D
7.1	1H	d	8.3	G
6.89-6.87	1H	m		C/D
4.9	1H	dd	12.2, 5.4	O
4.35	2H	q	7.1	H
4.25-4.21	2H	m		K
4.01	2H	s		J
3.9	2H	t	4.8	K
3.79-3.74	2H	m		K
3.70-3.62	2H	m		K
2.92	2H	t	5.4	K
2.87-2.61	3H	m		P
2.33	3H	s		A
2.09-2.03	1H	m		Q
1.43	3H	t	7.1	I

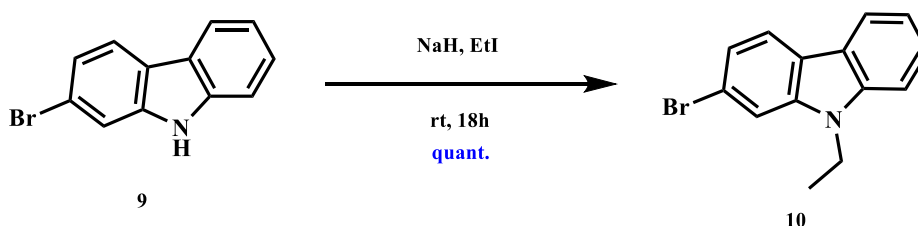
Table 8: ^1H NMR assignments for PROTAC 2. Assignment letters can be seen in figure 12.

Shift (ppm)	HSQC	Assignment
171.0	Q	R
168.2	Q	S
167.1	Q	N
165.8	Q	N
156.5	Q	L
145.4	Q	L
140.8	Q	L
140.0	Q	F
138.8	Q	B
136.5	Ar-CH	M
133.8	Q	E
132.5	Q	F
126.6	Ar-CH	G
125.6	Ar-CH	C/D
123.0	Q	F
122.4	Q	F
120.9	Ar-CH	G
120.4	Ar-CH	G
120.1	Ar-CH	C/D
119.5	Ar-CH	M
117.6	Ar-CH	G
117.4	Q	F
116.2	Ar-CH	G
108.5	Ar-CH	G
105.6	Ar-CH	M
71.2	CH ₂	K
70.5	CH ₂	K
70.3	CH ₂	K
69.4	CH ₂	K
69.4	CH ₂	K
54.2	CH ₂	J
49.3	CH	O
48.7	CH ₂	K
37.8	CH ₂	H
31.5	CH ₂	P
31.5	CH	Q
22.8	CH	Q
16.1	CH ₃	A
14	CH ₃	I

Table 9: ¹³C NMR assignments for PROTAC 2. HSQC was used to determine C environment. Where Q is quaternary carbon and Ar-CH is aromatic CH. Assignment letters can be seen in figure 12.

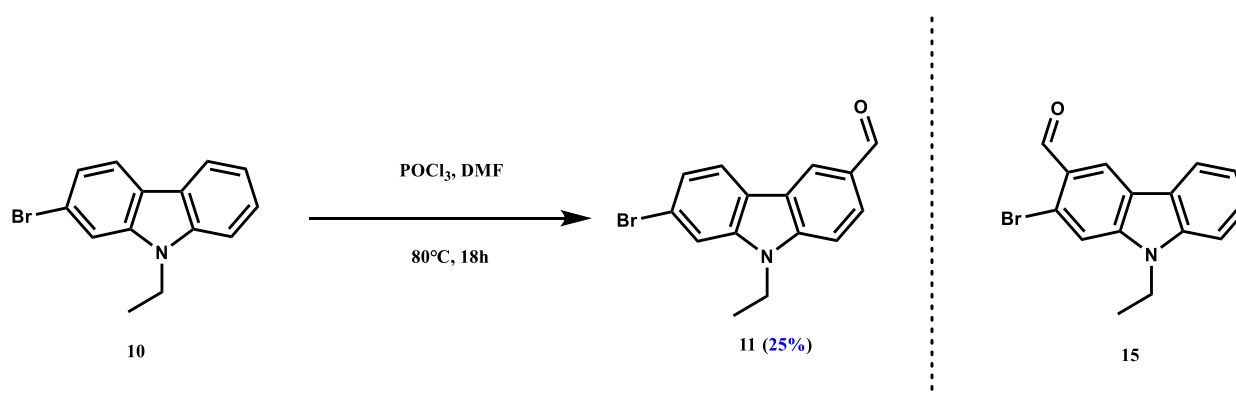
PK9328 warhead

The procedure for synthesis of PK9328 warhead **14** was adapted from literature precedent.²² The initial alkylation step in the synthetic route towards the PK9328 warhead **14** was successful, with quantitative yields achieved of ethyl carbazole **10** (Scheme 10).



Scheme 10: Synthesis of ethyl carbazole **10** through alkylation.

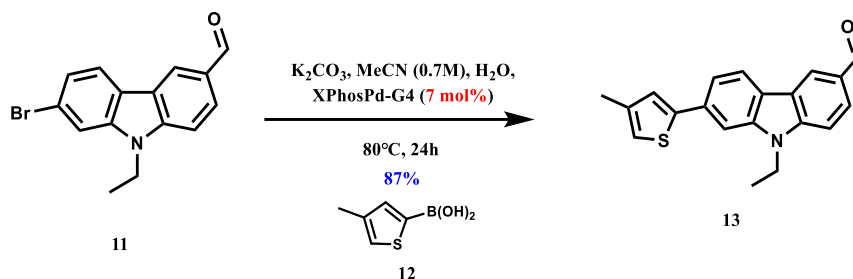
Next, a Vilsmeier-Haack reaction occurred in which **10** was reacted to give aldehyde **11**, along with aldehyde **15** as a side product in a 5:1 ratio, respectively. Both aldehyde **11** and **15** were separable by column chromatography, which allowed for isolation of aldehyde **11** with a 25% yield achieved (Scheme 11).



Scheme 11: Vilsmeier-Haack reaction of ethyl carbazole **10** to produce two aldehyde products **11** and **15** in a 5:1 ratio by ¹H NMR. Isolated yield of aldehyde **11** detailed in scheme.

The next step in the synthesis of PK9328 warhead **14** was a Suzuki cross-coupling reaction between aldehyde **11** and the boronic acid **12** (Figure 13). This reaction was required to reach full conversion as the starting material **11** and product **13** had the same *r_f* value, making separation of the two very difficult by column chromatography. To achieve full conversion, the catalyst loading of XPhosPd-G4 was altered from the initial addition of just 3 mol% of catalyst which reached only 84% conversion with 63% conversion observed within the first 0.5 h of the reaction. The optimal catalyst loading

was determined to be 7 mol%, which when added in three portions; 3 mol%, 3 mol% and 1 mol% gave full conversion to **13** in 87% yield (Figure 13 and 14).



Catalyst Loading of XPhosPd-G4	Conversion to 13 / %
3 mol%	84
6 mol% (3 mol% + 3 mol%)	90
7 mol% (3 mol% + 3 mol% + 1 mol%)	100

Figure 13: Suzuki cross-coupling reaction of aldehyde **11** with boronic acid **12**. Comparison of catalyst loading of XPhosPd-G4 with conversion to **13**. (Conversion measured using LCMS).

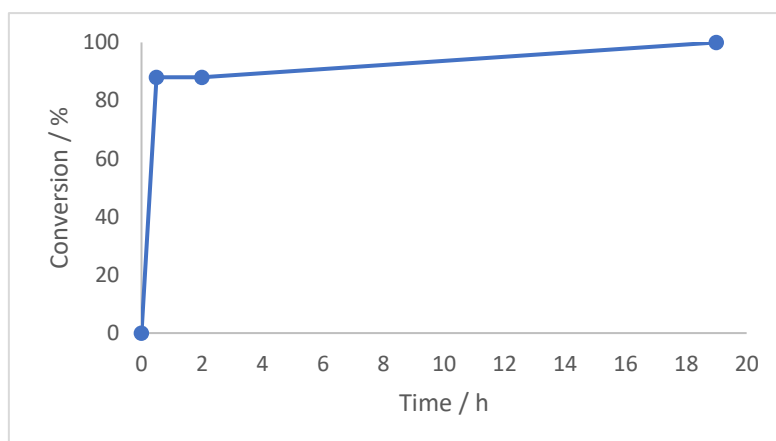
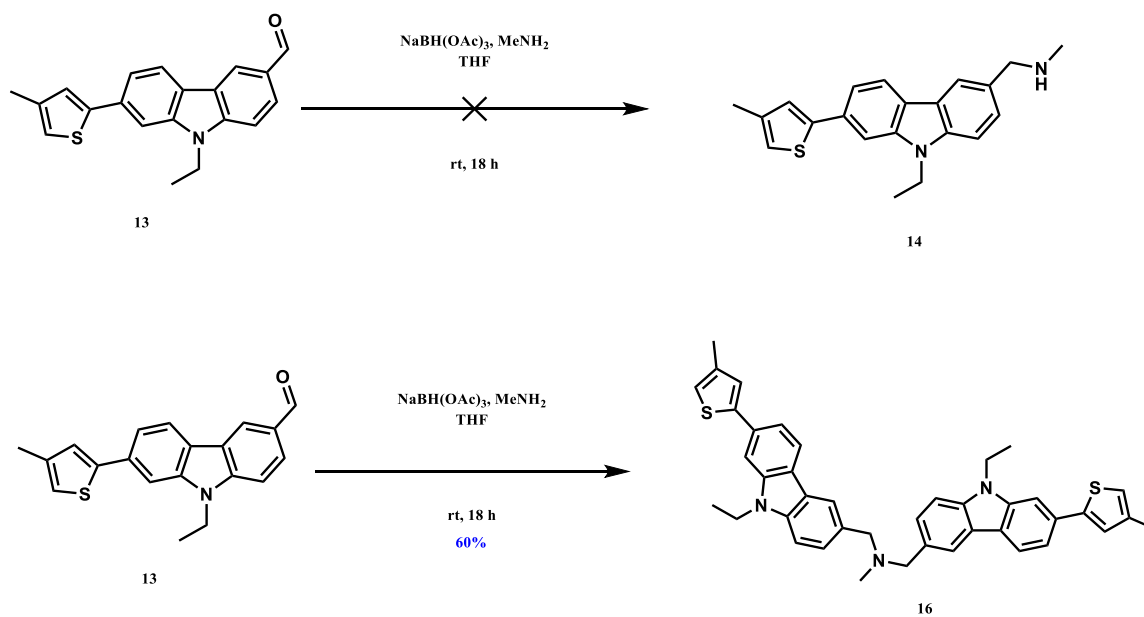


Figure 14: Conversion study of Suzuki cross-coupling of aldehyde **11** to product **13** using 7 mol% catalyst loading. (Conversion measured using LCMS).

Reductive amination of the Suzuki product **13** to the final PK9328 warhead **14** was unsuccessful, as it was discovered by NMR (Table 10 and 11) and HRMS that the dimer version **16** of warhead **14** had formed with a 60% yield achieved (Scheme 12). Further studies would have to take place in order to form the desired product **14**. Compound **16** was then submitted for biological testing.



Scheme 12: Formation of dimer **16** instead of monomer **14** through reductive amination of aldehyde **13**.

NMR Assignments for PK9328 warhead

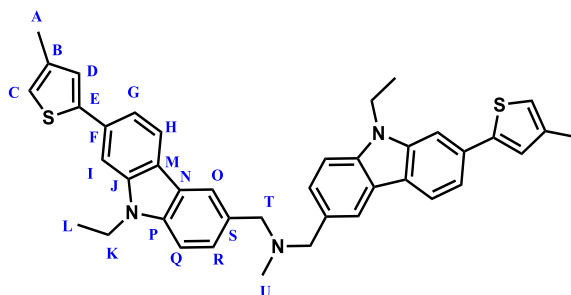


Figure 15: Structure of PK9328 warhead **16** with proton and carbon letter assignments.

Shift (ppm)	Integration	Multiplet	Assignment
8.09	1H	d	O
8.05	1H	d	Q
7.61-7.54	2H	m	I & G
7.49	1H	d	R
7.4	1H	d	H
7.25	1H	s	D
6.89	1H	s	C
4.39	2H	q	K
4.02	2H	s	T
2.43	2H	s	U
2.33	3H	s	A
1.46	3H	t	L

Table 10: ^1H NMR assignments for compound **16**. Assignment letters can be seen in figure 15.

Shift (ppm)	HSQC	Assignment
145.5	Q	M
141	Q	N
140.6	2 × Q	J and P
139	Q	B
132.8	Q	F
128.1	Ar-CH	I or G
125.8	Ar-CH	D
123.2	Q	E
122.4	Q	S
122.3	Ar-CH	O
121.1	Ar-CH	Q
120.3	Ar-CH	C
117.9	Ar-CH	R
108.9	Ar-CH	H
105.9	Ar-CH	I or G
61.4	CH ₂	T
40.8	CH ₃	U
38	CH ₂	K
16.2	CH ₃	A
14.2	CH ₃	L

Table 11: ^{13}C NMR assignments for compound **16**. HSQC was used to determine C environment. Where Q is quaternary carbon and Ar-CH is aromatic CH. Assignment letters seen in figure 15.

Biological testing of compounds

The biological testing of the PROTACs HM-I-37 (**1**) and HM-I-35 (**2**) and the PK9328 warhead HM-I-34 (**16**) was carried out at the CRUK-Beatson Institute. BxPC3 cells were used for this purpose as they endogenously express the p53 Y220C mutant. Partial degradation of the p53 Y220C mutant was observed when the cells were treated with 1 μM of HM-I-35 (**2**) with complete degradation observed at 25 μM (Figure 16). PROTAC HM-I-37 (**1**) displayed partial degradation of the p53 Y220C mutant at 25 μM , however, complete degradation was not observed at this concentration (Figure 16). It only achieved complete p53 Y220C degradation at $\sim 100 \mu\text{M}$. So, a significant improvement in the efficiency of PROTAC HM-I-35 (**2**), as compared to HM-I-37 (**1**) is observed. As expected, the PK9328 warhead HM-I-34 (**16**) showed no effect on the intracellular concentration of p53 Y220C mutant which demonstrates that degradation is PROTAC-dependent (Figure 16). The results show that PROTAC HM-I-35 (**2**) is a potent degrader of the p53 Y220C mutant at low micromolar concentration. This raises the possibility for the biological application of this PROTAC in p53 Y220C mutant context with little/no off-target effects.

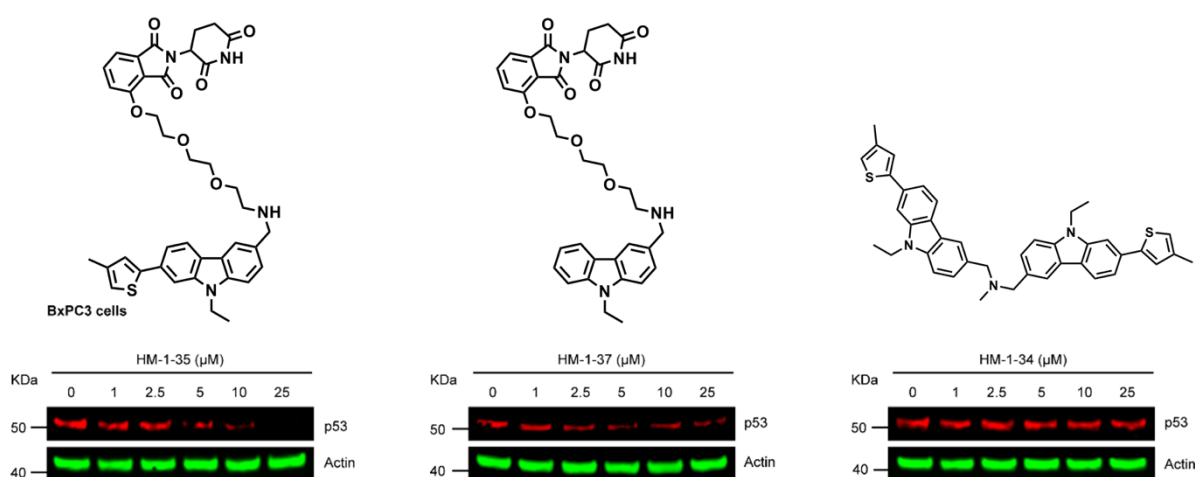


Figure 16: Immunoblots showing stability of p53 Y220C in mammalian cells. BxPC3 cells seeded onto 60 mm dishes were treated with the PROTACs HM-I-35 (**2**), HM-I-37 (**1**) and the PK9328 warhead HM-I-34 (**16**) as indicated. The immunoblots were analysed by anti-p53 (red) and anti-Actin (green) antibodies. Actin was used as the loading control. The molecular weights (KDa) have been indicated.

Conclusions and Future Work

The PROTACs HM-I-37 (**1**) and HM-I-35 (**2**) along with the PK9328 ligand, HM-I-34 (**16**) were successfully designed and synthesised and their biological activities against the Y220C p53 mutant were tested. PROTACs **1** and **2** and PK9328 ligand **16** were synthesised over four steps with overall yields of 6, 16 and 13%, respectively.

PROTAC HM-I-35 (**2**) was shown to be a degrader of the Y220C p53 mutant at concentrations as low as 1 μ M. Introduction of a methyl substituted thiophene on the POI ligand, as in PROTAC **2**, led to a 25-fold increase in degradation of Y220C p53 mutant in comparison to PROTAC **1**. This indicates that introduction of the methyl substituted thiophene has a significant impact on the degradative ability of the PROTAC, filling a previously unoccupied subsite of the Y220C binding pocket.

With PROTACs it is important to not only monitor degradation as a final process in the PROTAC degradation pathway but to also investigate the multi-step degradation pathway as a whole. Looking at the formation of binary and ternary complexes, which are often rate limiting processes, can aid in the development of potent PROTACs. One such assay which can probe the different steps in the PROTAC degradation pathway is the BRET assay which can utilise the NanoLuciferase enzyme and HaloTag protein to investigate these key processes leading to degradation of the POI.⁵⁸ Also, the use of a proteasome inhibitor, such as MG132, can demonstrate that degradation by the PROTAC is proteasome-mediated.⁵⁹

Future work could include the development of a PROTAC with a POI ligand based on the potent JC744 binder of Y220C p53 mutant, as this has been shown to bind with nanomolar affinity which is an improvement to that seen for the PK9328 binder for which PROTAC **2** is based on (Table 1).²³

Experimental

Chemistry Experimental

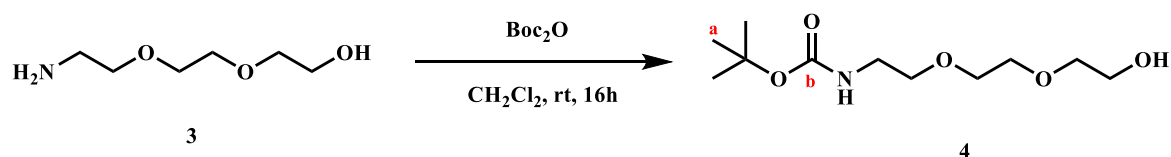
General Procedures

All reagents were purchased from commercial suppliers and used without further purification unless otherwise stated. Reactions requiring air-sensitive reagents and dry solvents were performed in glassware that had been dried in an oven at 150 °C prior to use. These reactions were carried out under argon atmosphere with the exclusion of air. Reactions were monitored by thin-layer chromatography (TLC) on Merck silica gel 60 covered aluminium sheets. TLC plates were visualised under UV-light, and where required with an acidic ethanolic anisaldehyde solution or a bromo-cresol green solution. NMR spectra were recorded on a Bruker DPX-400 spectrometer (^1H NMR at 400 MHz or ^{13}C NMR at 101 MHz). Chemical shifts are reported in ppm. ^1H NMR spectra were recorded with chloroform-*d* as the solvent using residual CHCl_3 ($\delta = 7.26$) as internal standard, and for ^{13}C NMR spectra the chemical shifts are reported relative to the central resonance of CDCl_3 ($\delta = 77.16$). Signals in the obtained spectra are reported as singlet (s), doublet (d), triplet (t), quartet (q), multiplet (m), broad (br), or a combination of these, to describe the observed spin–spin coupling pattern. Spin–spin coupling constants are reported in Hertz (Hz) and are uncorrected. Two-dimensional NMR spectroscopy (COSY, HSQC or HMBC) was employed where appropriate to assist the assignment of signals in the ^1H and ^{13}C NMR spectra. The selected assigned resonances were used to confirm connectivity or transformation. IR spectra were obtained on a Shimadzu FTIR-8400 instrument with a Golden Gate™ attachment using a type IIa diamond as a single reflection element for the IR spectra of the solid or liquid compounds to be detected directly (thin layer). High-resolution mass spectra (HRMS) were recorded using atmospheric pressure chemical ionisation (APCI) conditions by the analytical services at the University of Glasgow. Liquid chromatography–mass spectrometry (LCMS) was recorded on an Agilent 1260 Infinity II LC system coupled with an Agilent InfinityLab single quadrupole mass spectrometer using positive mode electrospray ionisation (ESI+) or negative mode electrospray ionisation (ESI-). A Shimadzu Shim-pack XR-ODS C18 2.2 μm 50 mm column was used with UV absorption detected at 214 nm and 254 nm. Linear gradients

between 10% to 90% HPLC-grade acetonitrile in ultra-pure water with 0.1% formic acid over 15 minutes were utilised with a flow rate of 1 mL min⁻¹. Semi-preparative reverse-phase HPLC was performed on a Gilson HPLC system equipped with Gilson 306 pumps, a Phenomenex Synergi C18 (80 Å, 10 µm, 250 x 21.2 mm) column at a flow rate of 8 mL min⁻¹. Non-linear gradients between 5% to 100% HPLC grade acetonitrile in ultra-pure water with 0.1% formic acid were utilised. UV absorption was detected at 214 nm and 254 nm using a Gilson 155 UV/VIS detector. Collected fractions were then lyophilised using Christ A 2-4 LO plus lyophiliser.

Preparation of compounds

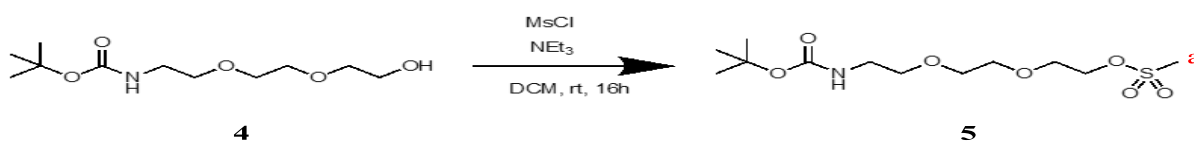
Preparation of PROTAC 1



4: Alcohol **3** (4.50 g, 30.2 mmol) was dissolved in a solution of anhydrous dichloromethane (101 mL, 0.3 M) under an argon atmosphere at 0 °C. Di-*tert*-butyl dicarbonate (6.57 g, 30.2 mmol) was added to the reaction mixture which was then stirred for 16 h at ambient temperature. The reaction mixture was then concentrated *in vacuo*. Purification of the crude material was performed by column chromatography on silica gel using an eluent of 50% ethyl acetate/pet ether to 100% ethyl acetate to afford the Boc protected linker **4** (4.25 g, 17.1 mmol) as a pale-yellow oil in 79% yield.

The analytical data observed were in accordance with the literature values.⁶⁰

¹H NMR (400 MHz, chloroform-*d*) δ 5.09 (1H, br s, NH), 3.77–3.73 (2H, m), 3.68–3.60 (6H, m), 3.56 (2H, t, J = 5.3 Hz), 3.35–3.30 (2H, m), 2.39 (1H, br s, OH), 1.44 (9H, s, 3 × CH₃^a). ¹³C NMR (101 MHz, chloroform-*d*) δ 156.1 (C^b=O), 79.5, 72.7, 70.6, 70.4, 61.9, 60.5, 40.5, 28.6, 21.2, 14.3. LCMS (ESI) mass calculated for C₁₁H₂₃NO₅ [M+Na]⁺ m/z 272.1, found m/z 272.1 with t_R = 0.83 min.

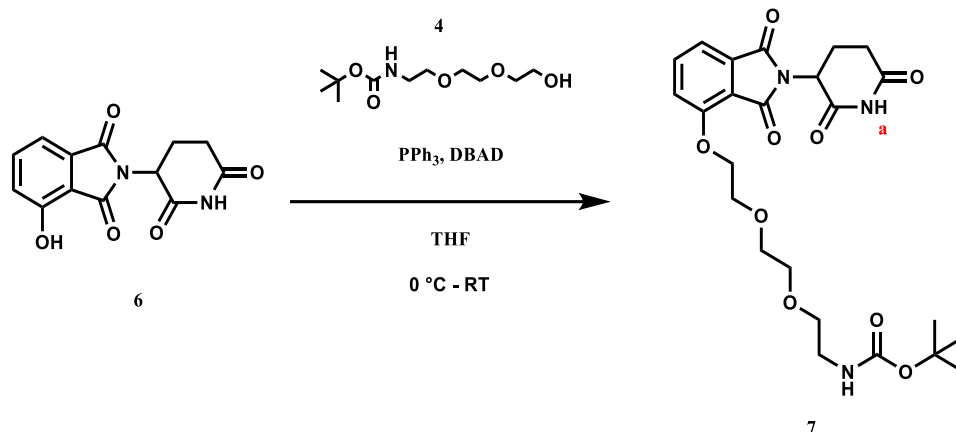


5: Boc-protected linker **4** (2.70 g, 10.8 mmol) was dissolved in anhydrous dichloromethane (54 mL, 0.2 M) with stirring under an argon atmosphere at ambient temperature. This was then followed by the addition of methane sulfonyl chloride (1.30 mL, 16.2 mmol) and triethylamine (2.25 mL, 16.2 mmol). The solution was then stirred for 16 h. The reaction mixture was concentrated *in vacuo* and redissolved in dichloromethane (20 mL). The solution was then washed with water (20 mL) and extracted with dichloromethane (3 × 20 mL). The resulting organic layers were dried over anhydrous MgSO₄ and remaining solvent removed *in vacuo* to afford **5** in quantitative yield (3.55 g, 10.8 mmol) as a dark yellow oil.

The crude material was used in the next step without need for further purification.

The analytical data observed was in accordance with the literature values.⁶¹

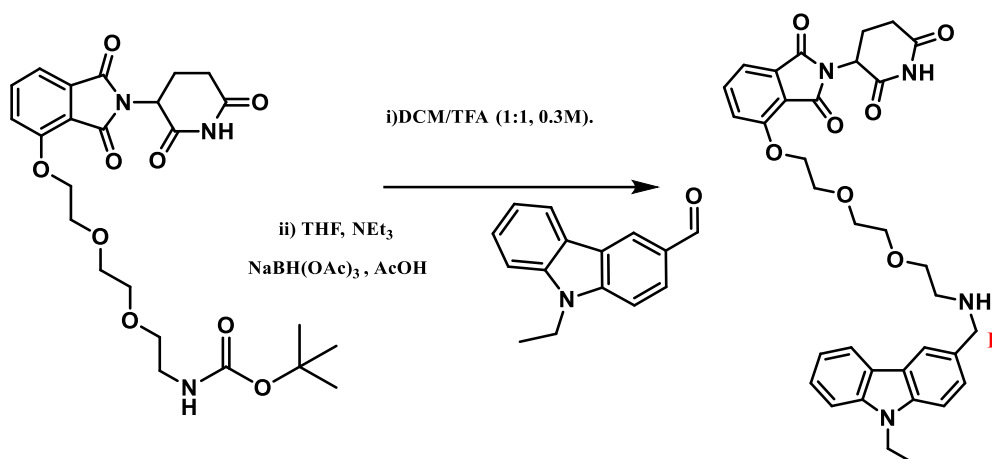
¹H NMR (400 MHz, chloroform-*d*) δ 4.92 (1H, s, NH), 4.40–4.36 (2H, m), 3.78–3.74 (2H, m), 3.68–3.64 (2H, m), 3.63–3.59 (2H, m), 3.52 (2H, t, J = 5.3 Hz), 3.33–3.27 (2H, m), 3.06 (3H, s, CH₃^a), 1.44 (9H, s, 3 × CH₃). ¹³C NMR (101 MHz, chloroform-*d*) δ 156.1 (C=O), 79.5, 70.7, 70.4, 70.3, 69.2 (2 × CH₂), 52.7, 40.5, 37.8, 28.5. LCMS (ESI) mass calculated for C₁₂H₂₅NO₇S [M+Na]⁺ m/z 350.1, found m/z 350.1 with t_R = 8.80 min.



7: To a dry flask charged with argon was added boc-protected linker **4** (100 mg, 0.40 mmol), CRBN ligand **6** (121 mg, 0.44 mmol) and triphenylphosphine (126 mg, 0.48 mmol) which was then dissolved in anhydrous tetrahydrofuran (4 mL, 0.1 M). The resulting solution was cooled to 0 °C before addition of di-tert-butyl azodicarboxylate (111 mg, 0.48 mmol). The solution was then stirred for 16 h. The reaction mixture was diluted with water (10 mL) and extracted with ethyl acetate (3 × 10 mL). The combined organic extracts were then washed with sodium bicarbonate (3 × 10 mL) to remove any remaining CRBN ligand, the solution was then dried over anhydrous MgSO₄, filtered and concentrated *in vacuo*. Purification of the crude material was performed by column chromatography on silica gel using an eluent of 1% methanol/dichloromethane to 3% methanol/dichloromethane to afford the desired alkylated product **7** (146 mg, 0.29 mmol) as a white solid in 72% yield.

The analytical data observed was in accordance with the literature values.⁵⁵

¹H NMR (400 MHz, chloroform-*d*) δ 8.17 (1H, s, NH^a), 7.68 (1H, dd, *J* = 8.2, 7.6 Hz, Ar-CH), 7.48 (1H, d, *J* = 7.3 Hz, Ar-CH), 7.26 (1H, d, *J* = 8.4 Hz, Ar-CH), 5.02–4.92 (2H, m), 4.35 (2H, t, *J* = 4.7 Hz), 3.95 (2H, t, *J* = 4.7 Hz), 3.78 (2H, m), 3.63 (2H, t, *J* = 4.9 Hz), 3.55 (2H, t, *J* = 4.9 Hz), 3.34–3.27 (2H, m), 2.93–2.67 (3H, m), 2.15–2.09 (1H, m), 1.43 (9H, s, 3 × CH₃). ¹³C NMR (101 MHz, chloroform-*d*) δ 171.1, 168.3, 167.1, 156.5, 156.2, 136.6, 133.9, 119.5, 117.5, 116.3, 79.4, 71.3, 70.4 (2 × CH₂), 69.5 (2 × CH₂), 53.6, 49.3, 40.5, 31.5, 28.6, 22.8. LCMS (ESI) mass calculated for C₂₄H₃₁N₃O₉ [M+Na]⁺ *m/z* 528.2, found *m/z* 528.1 with *t_R* = 1.732 min.

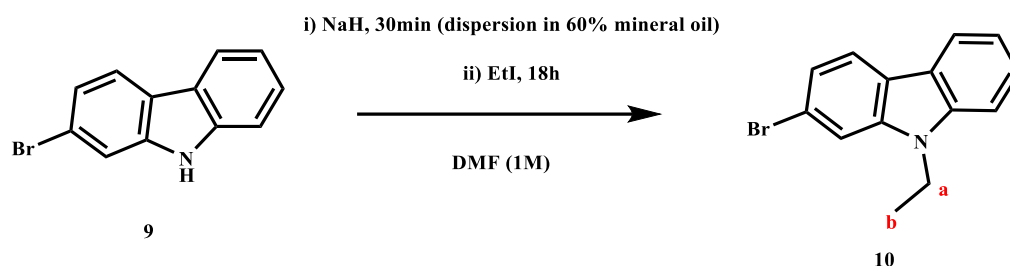


PROTAC 1: The boc-protected CRBN linker **7** (50 mg, 0.1 mmol) was dissolved in trifluoroacetic acid/dichloromethane (0.5 mL/0.5 mL, 0.3 M) and the resulting solution was stirred at ambient temperature for 1 h. The reaction mixture was then concentrated *in vacuo* to remove volatile components. To the resulting residue was added anhydrous tetrahydrofuran (1.9 mL, 0.05 M) and triethylamine (0.06 mL, 0.4 mmol) under an argon atmosphere and the resulting solution was stirred for 10 minutes. To this solution was added aldehyde **8** (22 mg, 0.1 mmol), sodium triacetoxyborohydride (127 mg, 0.6 mmol) and acetic acid (0.03 mL, 0.6 mmol) and the reaction mixture stirred for 24 h. The reaction mixture was diluted in dichloromethane (15 mL) and the solution washed with saturated aqueous sodium bicarbonate (3 × 15 mL). The organic extracts were combined, dried over anhydrous MgSO₄, filtered and concentrated *in vacuo*. Purification of the crude material was performed by column chromatography on silica gel using an eluent of 5% methanol/dichloromethane to 7% methanol/dichloromethane to afford **PROTAC 1** (6.5 mg, 0.01 mmol) as a white solid in 11% yield.

¹H NMR (400 MHz, chloroform-*d*) δ 8.09–8.03 (2H, m), 7.54 (1H, dd, *J* = 8.4, 7.3 Hz, Ar-CH), 7.48–7.37 (4H, m), 7.34 (1H, d, *J* = 8.4 Hz, Ar-H), 7.20 (1H, ddd, *J* = 8.4, 7.1, 1.0 Hz, Ar-CH), 7.12 (1H, d, *J* = 8.4 Hz, Ar-CH), 4.90 (1H, dd, *J* = 12.0, 5.2 Hz), 4.34 (2H, q, *J* = 7.2 Hz), 4.25 (2H, t, *J* = 4.5 Hz), 3.99 (2H, s, CH₂^F), 3.92–3.89 (2H, m), 3.79–3.75 (2H, m), 3.67–3.61 (4H, m), 2.89 (2H, t, *J* = 5.4 Hz), 2.86–2.60 (3H, m), 2.10–2.02 (1H, m), 1.41 (3H, t, *J* = 7.2 Hz). ¹³C NMR (101 MHz, chloroform-*d*) δ 171.0, 168.2, 167.1, 165.7, 156.5, 140.3, 139.4, 136.5, 133.8, 130.4, 126.5, 125.7, 123.1, 122.9, 120.6, 120.4, 119.6, 118.9, 117.4, 116.2, 108.6, 108.4, 71.2, 70.5, 69.5, 69.4, 54.3 (CH₂^F), 49.2, 48.7, 37.7, 31.5 (1 × CH₂ and 1 × CH), 22.8, 14.0. HRMS (APCI)

exact mass calculated for $C_{34}H_{36}N_4O_7$ $[M+H]^+$ m/z 613.2657, found m/z 613.2667. LCMS (ESI) mass calculated for $C_{34}H_{36}N_4O_7$ $[M+H]^+$ m/z 613.3, found m/z 613.3 with $t_R = 2.863$ min. ν_{max}/cm^{-1} (neat) 2924 (CH), 2856 (CH), 1712 (CO), 1488, 1470, 1395, 1350, 1264, 1232, 1201, 1128, 749.

Preparation of PROTAC 2

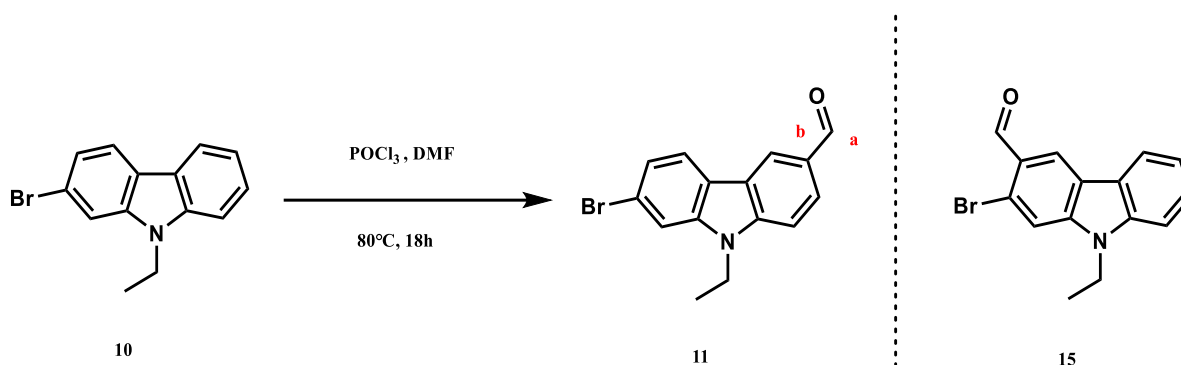


10: 2-Bromocarbazole **9** (5.00 g, 20.4 mmol) was dissolved in anhydrous N,N-dimethyl formamide (20 mL, 1 M). Sodium hydride (1.62 g, 40.6 mmol) was added to the solution at 0 °C and the reaction stirred for 1 h at room temperature. To the reaction mixture was added ethyl iodide (3.30 mL, 40.6 mmol) dropwise at 0 °C. The reaction was stirred for 18 h at room temperature. The reaction mixture was quenched by dropwise addition of water (20 mL). The resulting solution was extracted with ethyl acetate (3 × 20 mL). The combined organic extracts were then washed with brine (3 × 20 mL), dried over anhydrous $MgSO_4$, filtered and concentrated *in vacuo*. This afforded the product aryl bromide **10** (5.58 g, 20.4 mmol) in quantitative yield as a beige crystalline solid.

The crude material was used in the next step without need for further purification.

The analytical data observed was in accordance with the literature values.⁶²

1H NMR (400 MHz, chloroform-*d*) δ 8.07 (1H, d, $J = 7.8$ Hz, Ar-CH), 7.94 (1H, d, $J = 8.2$ Hz, Ar-CH), 7.56 (1H, s, Ar-CH), 7.49 (1H, t, $J = 8.1$ Hz, Ar-CH), 7.41 (1H, d, $J = 8.2$ Hz, Ar-CH), 7.33 (1H, d, $J = 8.2$ Hz, Ar-CH), 7.25 (1H, m, Ar-CH), 4.34 (2H, q, $J = 7.2$ Hz, CH_2^a), 1.44 (3H, t, $J = 7.3$ Hz, CH_3^b). ^{13}C NMR (101 MHz, chloroform-*d*) δ 140.9, 140.2, 126.2, 122.6, 122.0, 121.8, 120.6, 119.5, 119.4, 111.7, 108.8, 37.8 (C^aH_2), 13.9 (C^bH_3). LRMS (APCI) mass calculated for $C_{14}H_{12}BrN$ $[M+H]^+$ m/z 274.0, found m/z 274.0.

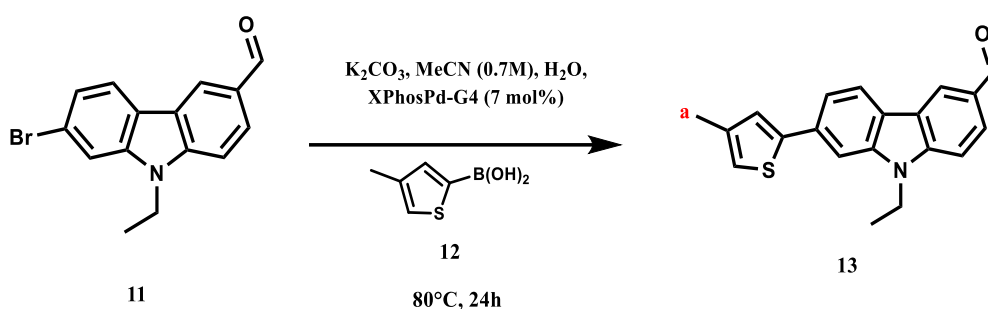


11: Phosphorous(V) oxychloride (2.70 mL, 29.43 mmol) was added dropwise to a solution of anhydrous *N, N*-dimethyl formamide (4.95 mL, 2 M) in a dry flask under an argon atmosphere at 0 °C. The resulting solution was stirred for 1 h at ambient temperature. To this solution was then added aryl bromide **10** (2.70 g, 9.84 mmol) the resulting mixture was left to stir for 18 h under an argon atmosphere at 80 °C. The reaction mixture was cooled to room temperature before being quenched with ice water (20 mL). To the mixture was then added 10% w/v aqueous NaOH_(aq) until tested neutral to litmus paper. The crude product was then extracted with ethyl acetate (3 × 20 mL). The organic layers were then combined and washed with brine (3 × 20 mL), dried over anhydrous MgSO₄ and concentrated *in vacuo*. Purification of the crude material was performed by column chromatography on silica gel using an eluent of 5% ethyl acetate/petroleum ether to afford aldehyde **11** (746 mg, 2.47 mmol) as a beige solid in 25% yield.

The analytical data observed was in accordance with the literature values.⁶²

11: ¹H NMR (400 MHz, chloroform-*d*) δ 10.10 (1H, s, CH^aO), 8.58 (1H, s, Ar-CH), 8.03 (1H, d, *J* = 7.1 Hz, Ar-CH), 8.00 (1H, d, *J* = 8.2 Hz, Ar-CH), 7.61 (1H, s, Ar-CH), 7.48 (1H, d, *J* = 8.7 Hz, Ar-CH), 7.43 (1H, d, *J* = 8.2 Hz, Ar-CH), 4.37 (2H, q, *J* = 7.3 Hz, CH₂), 1.47 (3H, t, *J* = 7.3 Hz, CH₃). ¹³C NMR (101 MHz, chloroform-*d*) δ 191.8 (C^b=O), 143.9, 141.8, 129.3, 127.8, 124.1, 123.8, 122.9, 122.3, 122.2, 120.6, 112.6, 109.2, 38.4, 14.0 (CH₃). LCMS (ESI) mass calculated for C₁₅H₁₂BrNO [M+H]⁺ *m/z* 302.2, found *m/z* 302.0 with *t_R* = 9.50 min.

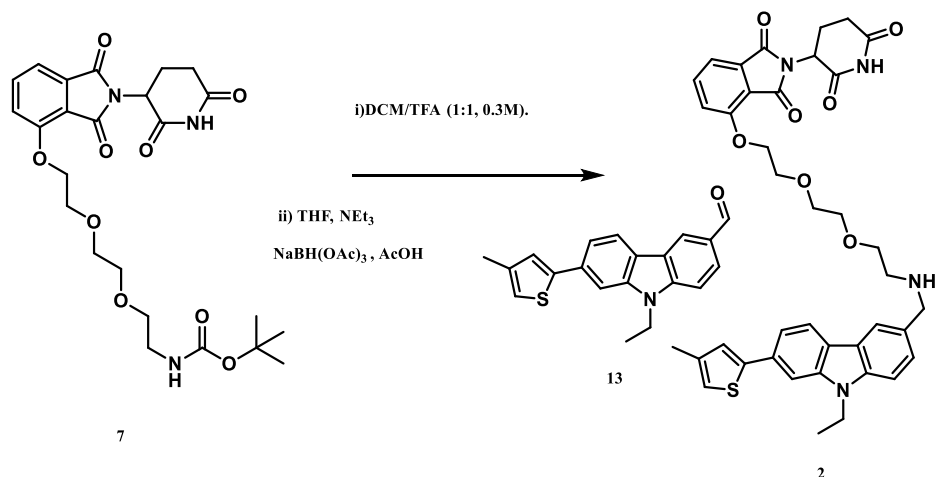
15: ^1H NMR (400 MHz, chloroform-*d*) δ 10.45 (1H, s, CHO), 8.71 (1H, s), 8.13 (1H, dt, $J = 7.8, 1.0$ Hz, Ar-CH), 7.61 (1H, s, Ar-CH), 7.55 (1H, ddd, $J = 8.3, 7.2, 1.2$ Hz, Ar-CH), 7.44 (1H, dt, $J = 8.2, 0.9$ Hz, Ar-CH), 7.33 (1H, ddd, $J = 8.0, 7.1, 1.0$ Hz, Ar-CH), 4.36 (2H, q, $J = 7.3$ Hz, CH_2), 1.48 (3H, t, $J = 7.3$ Hz, CH_3). ^{13}C NMR (101 MHz, chloroform-*d*) δ 192.0, 144.0, 141.0, 127.4, 125.1, 124.3, 123.1, 123.0, 122.9, 121.3, 121.0, 112.9, 109.4, 38.2, 13.9.



13: Water (1 mL, 0.7 M) and acetonitrile (1 mL, 0.7 M) were degassed under argon for 0.5 h. To a dry flask under an argon atmosphere was added aldehyde **11** (200 mg, 0.66 mmol), potassium carbonate (182 mg, 1.32 mmol), XPhosPd-G4 (15 mg, 0.02 mmol) and boronic acid **12** (112 g, 0.79 mmol). The degassed water and acetonitrile were then added to the flask and the reaction mixture stirred for 2 h at 80°C . A further portion of catalyst, XPhosPd-G4 (15 mg, 0.02 mmol), was then added to the reaction mixture and the reaction stirred for a further 17 h. A final portion of catalyst, XPhosPd-G4 (5 mg, 0.007 mmol) was added to the reaction mixture and the reaction stirred for a further 1 h. The reaction mixture was left to cool to ambient temperature, then diluted by addition of water (10 mL) and the crude product extracted with ethyl acetate (3×10 mL). The organic extracts were then combined and washed with brine (10 mL), dried over anhydrous MgSO_4 , filtered and concentrated *in vacuo*. Purification of the crude product was performed by column chromatography on silica gel using an eluent of 10% ethyl acetate in petroleum ether to afford the desired biaryl aldehyde **13** (229 mg, 0.72 mmol) as a yellow solid in 87% yield.

The analytical data observed was in accordance with the literature values.⁶²

^1H NMR (400 MHz, chloroform-*d*) δ 10.10 (1H, s, CHO), 8.59 (1H, s, Ar-H), 8.12 (1H, d, $J = 8.1$ Hz, Ar-H), 8.01 (1H, d, $J = 8.5$ Hz, Ar-H), 7.62 (1H, s, Ar-H), 7.57 (1H, d, $J = 8.7$ Hz, Ar-H), 7.48 (1H, d, $J = 8.3$ Hz, Ar-H), 6.92 (1H, s, Ar-H), 4.44 (2H, q, $J = 7.2$ Hz, CH_2), 2.34 (3H, s, CH_3^a), 1.51 (3H, t, $J = 7.2$ Hz, CH_3). ^{13}C NMR (101 MHz, chloroform-*d*) δ 191.9, 144.8, 144.3, 141.3, 139.0, 133.6, 128.9, 127.4, 126.0, 124.0, 123.2, 122.5, 121.3, 120.6, 119.0, 108.9, 106.2, 38.1, 16.1, 14.0. LCMS (ESI) mass calculated for $\text{C}_{20}\text{H}_{17}\text{NOS}$ $[\text{M}+\text{H}]^+$ m/z 320.2, found m/z 320.1 with $t_R = 12.00$ min.

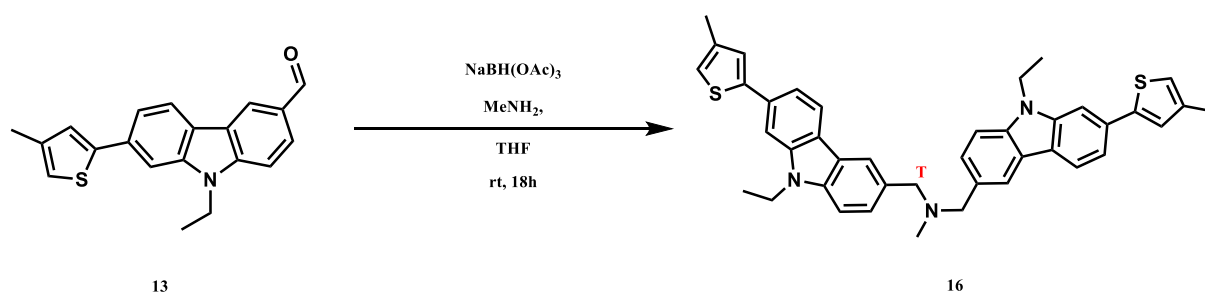


PROTAC 2: Boc-protected CRBN ligand **7** (50 mg, 0.1 mmol) was dissolved in trifluoroacetic acid/dichloromethane (0.5 mL/0.5 mL, 0.3 M) and the resulting solution was stirred at ambient temperature for 1 h. The reaction mixture was then concentrated *in vacuo* to remove volatile components. To the resulting residue was added anhydrous tetrahydrofuran (1.9 mL, 0.05 M) and triethylamine (0.06 mL, 0.4 mmol) under an argon atmosphere and the resulting solution was stirred for 10 minutes. To this solution was added biaryl aldehyde **13** (32 mg, 0.1 mmol), sodium triacetoxyborohydride (127 mg, 0.6 mmol) and acetic acid (0.03 mL, 0.6 mmol) and the reaction mixture stirred for 17 h. The reaction mixture was diluted in dichloromethane (15 mL) and the solution washed with saturated aqueous sodium bicarbonate (3 \times 15 mL). The organic extracts were combined, dried over anhydrous MgSO_4 , filtered and concentrated *in vacuo*. Purification of the crude material was performed by column chromatography on silica gel using an eluent of 5% methanol/dichloromethane to 10% methanol/dichloromethane to afford the desired product **2** (20 mg, 0.03 mmol) as a beige solid in 28% yield.

^1H NMR (400 MHz, chloroform-*d*) δ 8.06-7.99 (2H, m, Ar-CH), 7.55-7.50 (2H, m, Ar-CH), 7.44 (2H, ddd, $J = 9.5, 6.2, 1.4$ Hz, Ar-CH), 7.39 (1H, d, $J = 7.0$ Hz, Ar-CH), 7.32 (1H, d, $J = 8.3$ Hz, Ar-CH), 7.23-7.22 (1H, d, $J = 1.2$ Hz, Ar-CH), 7.10 (1H, d, $J = 8.3$ Hz, Ar-CH), 6.89-6.87 (1H, m, Ar-CH), 4.90 (1H, dd, $J = 12.2, 5.4$ Hz, CH^a), 4.35 (2H, q, $J = 7.1$ Hz, CH₂), 4.25-4.21 (2H, m, CH₂), 4.01 (2H, s, CH₂^J), 3.90 (2H, t, $J = 4.8$, CH₂), 3.79-3.74 (2H, m, CH₂), 3.70-3.62 (2H, m, CH₂), 2.92 (2H, t, $J = 5.4$ Hz, CH₂), 2.87-2.61 (3H, m), 2.33 (3H, s, CH₃), 2.09-2.03 (1H, m), 1.43 (3H, t, $J = 7.1$ Hz, CH₃).

^{13}C NMR (101 MHz, chloroform-*d*) δ 171.0, 168.2, 167.1, 165.8, 156.5, 145.4, 140.8, 140.0, 138.8, 136.5, 133.8, 132.5, 126.6, 125.6, 123.0, 122.4, 120.9, 120.4, 120.1, 119.2, 117.6, 117.4, 116.2, 108.5, 105.6, 71.2, 70.5, 70.3, 69.4 (2 \times CH₂), 54.2 (CH₂^J), 49.3, 48.7, 37.8, 31.5 (1 \times CH₂ and 1 \times CH), 22.8, 16.1, 14.0. HRMS (APCI) exact mass calculated for C₃₉H₄₀N₄O₇S [M+H]⁺ m/z 709.2691, found m/z 709.2701. LCMS (ESI) mass calculated for C₃₉H₄₀N₄O₇S [M+H]⁺ m/z 709.3, found m/z 709.3 with $t_R = 7.957$ min. $\nu_{\text{max}}/\text{cm}^{-1}$ (neat) 2926 (CH), 2851 (CH), 1710 (CO), 1482, 1393, 1347, 1260, 1196, 1128, 1051, 729.

Preparation of parent compound for PROTAC 2



16: To a solution of biaryl aldehyde **13** (50 mg, 0.16 mmol) in anhydrous tetrahydrofuran (0.8 mL, 0.2 M) was added methylamine (0.1 mL, 2 M solution in THF, 0.24 mmol) and sodium triacetoxyborohydride (85 mg, 0.40 mmol) under an argon atmosphere. The resulting solution was stirred for 18 h at ambient temperature. The tetrahydrofuran was then removed *in vacuo*. The residue was then diluted with water (10 mL) and the crude product extracted with dichloromethane (10 mL), dried with anhydrous MgSO_4 , filtered and then concentrated *in vacuo*. The crude product was then purified using column chromatography on silica gel with an eluent of 5% methanol/dichloromethane to afford the desired product **16** (16 mg, 0.0 mmol) as a beige solid in 60% yield.

The analytical data observed was in accordance with the literature values.⁶²

^1H NMR (400 MHz, chloroform-*d*) δ 8.09 (1H, d, $J = 1.5$ Hz, Ar-H), 8.05 (1H, d, $J = 8.1$ Hz, Ar-H), 7.61–7.54 (2H, m, Ar-H), 7.49 (1H, dd, $J = 8.1, 1.5$ Hz, Ar-H), 7.40 (1H, d, $J = 8.7$ Hz, Ar-H), 7.25 (1H, s, Ar-H), 6.89 (1H, s, Ar-H), 4.39 (2H, q, $J = 7.2$ Hz, CH_2), 4.02 (2H, s, CH_2^{T}), 2.43 (2H, s, CH_2), 2.33 (3H, s), 1.46 (3H, t, $J = 7.1$ Hz). ^{13}C NMR (101 MHz, chloroform-*d*) δ 145.5, 141.0, 140.6 (2 \times C), 139.0, 132.8, 128.1, 125.8, 123.2, 122.4, 122.3, 121.1, 120.3, 117.9, 108.9, 105.9, 61.4, 40.8, 38.0, 16.2, 14.2. HRMS (APCI) exact mass calculated for $\text{C}_{41}\text{H}_{39}\text{N}_3\text{S}_2$ $[\text{M} + \text{H}]^+$ m/z 638.2658, found m/z 638.2670. LCMS (ESI) mass calculated for $\text{C}_{41}\text{H}_{39}\text{N}_3\text{S}_2$ $[\text{M} + \text{H}]^+$ m/z 638.3, found m/z 638.3 with $t_{\text{R}} = 2.790$ min.

Cell Biology Materials and Methods

Mammalian cell culture

The mammalian pancreatic cancer cell line BxPC3 (p53 Y220C) was used for cell-based assays. The cell line was cultured in RPMI-1640 medium which was supplemented with 10% FBS, 100 units/mL penicillin, 0.1 mg/mL streptomycin, 20 mM L-glutamine and 6 mg/L gentamycin (Invitrogen, USA) at 37°C in a humidified incubator with 5% CO₂. The cell line was tested for mycoplasma and authenticated using the GenePrint 10 System short tandem repeat profiling (Promega) in-house at the CRUK-Beatson Institute.

PROTACs and Immunoblotting

The PROTACs HM-I-35 and HM-I-37 and the ligand HM-I-34 were each made into a 7mM DMSO stock solution and the cells treated at final concentrations of 0, 1, 2.5, 5, 10 and 25 µM (Figure 11). The preparation of whole cell lysates was achieved through resuspending the cell pellets in lysis buffer (5 mM Tris-HCl pH 7.5, 150 mM NaCl, 1mM EDTA, 1% IGEPAL CA-630, 10% glycerol, 0.5 mM DTT and a protease inhibitor cocktail) which was then followed by immunoblotting. Briefly, SDS-PAGE was used to separate the protein samples using NuPAGE™ 4–12% Bis-Tris gels (Thermo Fisher Scientific) in MES-SDS running buffer. The proteins samples were then transferred onto nitrocellulose membranes using a Trans-Blot® Turbo™ Transfer System (Bio-Rad). The primary antibodies: rabbit anti-p53 (Cell Signalling), mouse anti-actin (Santa Cruz Biotechnology); and secondary antibodies: goat anti-rabbit IRDye 680LT (LI-COR Biosciences) and goat anti-mouse IRDye 800CW (LI-COR Biosciences) were used for probing the blots. The immunoblots were then scanned using the CLx Imaging System (LI-COR Biosciences Odyssey).

References

- 1 Cancer, <https://www.who.int/news-room/fact-sheets/detail/cancer>, (accessed 22 August 2023).
- 2 Global Cancer Observatory, <https://gco.iarc.fr/>, (accessed 22 August 2023).
- 3 Worldwide cancer risk factors | Cancer Research UK, <https://www.cancerresearchuk.org/health-professional/cancer-statistics/worldwide-cancer/risk-factors#heading-Zero>, (accessed 22 August 2023).
- 4 H. Sung, J. Ferlay, R. L. Siegel, M. Laversanne, I. Soerjomataram, A. Jemal and F. Bray, *CA. Cancer J. Clin.*, 2021, **71**, 209–249.
- 5 S. Zhang, L. Carlsen, L. Hernandez Borrero, A. A. Seyhan, X. Tian and W. S. El-Deiry, *Biomolecules*, 2022, **12**, 548.
- 6 J. J. Miller, C. Gaiddon and T. Storr, *Chem. Soc. Rev.*, 2020, **49**, 6995–7014.
- 7 M. Konopleva, G. Martinelli, N. Daver, C. Papayannidis, A. Wei, B. Higgins, M. Ott, J. Mascarenhas and M. Andreeff, *Leukemia*, 2020, **34**, 2858–2874.
- 8 X. Wu, J. H. Bayle, D. Olson and A. J. Levine, *Genes Dev.*, 1993, **7**, 1126–1132.
- 9 M. J. Duffy, N. C. Synnott, S. O’Grady and J. Crown, *Semin. Cancer Biol.*, 2022, **79**, 58–67.
- 10 H. Wang, M. Guo, H. Wei and Y. Chen, *Signal Transduct. Target. Ther.*, 2023, **8**, 92.
- 11 C. J. Brown, S. Lain, C. S. Verma, A. R. Fersht and D. P. Lane, *Nat. Rev. Cancer*, 2009, **9**, 862–873.
- 12 S. Nishikawa and T. Iwakuma, *Cancers (Basel)*, 2023, **15**, 429.
- 13 W. A. Freed-Pastor and C. Prives, *Genes Dev.*, 2012, **26**, 1268–1286.
- 14 G. Zhu, C. Pan, J.-X. Bei, B. Li, C. Liang, Y. Xu and X. Fu, *Front. Oncol.*, , DOI:10.3389/fonc.2020.595187.
- 15 A. C. Joerger and A. R. Fersht, *Oncogene*, 2007, **26**, 2226–2242.
- 16 A. C. Joerger and A. R. Fersht, *Annu. Rev. Biochem.*, 2008, **77**, 557–582.
- 17 A. C. Joerger, H. C. Ang and A. R. Fersht, *Proc. Natl. Acad. Sci.*, 2006, **103**, 15056–15061.
- 18 S. M. A. Rauf, A. Endou, H. Takaba and A. Miyamoto, *Protein J.*, 2013, **32**, 68–74.
- 19 J. Huang, *Pharmacol. Ther.*, 2021, **220**, 107720.
- 20 M. J. Duffy and J. Crown, *Int. J. Cancer*, 2021, **148**, 8–17.
- 21 F. M. Boeckler, A. C. Joerger, G. Jaggi, T. J. Rutherford, D. B. Veprintsev and

- A. R. Fersht, *Proc. Natl. Acad. Sci.*, 2008, **105**, 10360–10365.
- 22 M. R. Bauer, R. N. Jones, R. K. Tareque, B. Springett, F. A. Dingler, L. Verduci, K. J. Patel, A. R. Fersht, A. C. Joerger and J. Spencer, *Future Med. Chem.*, 2019, **11**, 2491–2504.
- 23 J. R. Stephenson Clarke, L. R. Douglas, P. J. Duriez, D.-I. Balourdas, A. C. Joerger, R. Khadiullina, E. Bulatov and M. G. J. Baud, *ACS Pharmacol. Transl. Sci.*, 2022, **5**, 1169–1180.
- 24 D. Nandi, P. Tahiliani, A. Kumar and D. Chandu, *J. Biosci.*, 2006, **31**, 137–155.
- 25 J. Bremner, 2015.
- 26 S. Aggarwal, P. Tolani, S. Gupta and A. K. Yadav, 2021, pp. 93–126.
- 27 L. Bedford, J. Lowe, L. R. Dick, R. J. Mayer and J. E. Brownell, *Nat. Rev. Drug Discov.*, 2011, **10**, 29–46.
- 28 M. Pettersson and C. M. Crews, *Drug Discov. Today Technol.*, 2019, **31**, 15–27.
- 29 J. Lu, Y. Qian, M. Altieri, H. Dong, J. Wang, K. Raina, J. Hines, J. D. Winkler, A. P. Crew, K. Coleman and C. M. Crews, *Chem. Biol.*, 2015, **22**, 755–763.
- 30 L. Zhao, J. Zhao, K. Zhong, A. Tong and D. Jia, *Signal Transduct. Target. Ther.*, 2022, **7**, 113.
- 31 T. Wu, H. Yoon, Y. Xiong, S. E. Dixon-Clarke, R. P. Nowak and E. S. Fischer, *Nat. Struct. Mol. Biol.*, 2020, **27**, 605–614.
- 32 K. T. G. Samarasinghe and C. M. Crews, *Cell Chem. Biol.*, 2021, **28**, 934–951.
- 33 K. M. Sakamoto, K. B. Kim, A. Kumagai, F. Mercurio, C. M. Crews and R. J. Deshaies, *Proc. Natl. Acad. Sci.*, 2001, **98**, 8554–8559.
- 34 S. Gu, D. Cui, X. Chen, X. Xiong and Y. Zhao, *BioEssays*, 2018, **40**, 1700247.
- 35 M. Xi, Y. Chen, H. Yang, H. Xu, K. Du, C. Wu, Y. Xu, L. Deng, X. Luo, L. Yu, Y. Wu, X. Gao, T. Cai, B. Chen, R. Shen and H. Sun, *Eur. J. Med. Chem.*, 2019, **174**, 159–180.
- 36 M. J. Bond and C. M. Crews, *RSC Chem. Biol.*, 2021, **2**, 725–742.
- 37 M. Békés, D. R. Langley and C. M. Crews, *Nat. Rev. Drug Discov.*, 2022, **21**, 181–200.
- 38 I. Churcher, *J. Med. Chem.*, 2018, **61**, 444–452.
- 39 A. D. Buhimschi, H. A. Armstrong, M. Toure, S. Jaime-Figueroa, T. L. Chen, A. M. Lehman, J. A. Woyach, A. J. Johnson, J. C. Byrd and C. M. Crews, *Biochemistry*, 2018, **57**, 3564–3575.
- 40 A. Bricelj, C. Steinebach, R. Kuchta, M. Gütschow and I. Sosič, *Front. Chem.*, , DOI:10.3389/fchem.2021.707317.
- 41 I. Sosič, A. Bricelj and C. Steinebach, *Chem. Soc. Rev.*, 2022, **51**, 3487–3534.
- 42 T. Ishida and A. Ciulli, *SLAS Discov.*, 2021, **26**, 484–502.

- 43 M. Konstantinidou, J. Li, B. Zhang, Z. Wang, S. Shaabani, F. Ter Brake, K. Essa and A. Dömling, *Expert Opin. Drug Discov.*, 2019, **14**, 1255–1268.
- 44 S. Khan, Y. He, X. Zhang, Y. Yuan, S. Pu, Q. Kong, G. Zheng and D. Zhou, *Oncogene*, 2020, **39**, 4909–4924.
- 45 C. A. Lipinski, F. Lombardo, B. W. Dominy and P. J. Feeney, *Adv. Drug Deliv. Rev.*, 1997, **23**, 3–25.
- 46 H. J. Maple, N. Clayden, A. Baron, C. Stacey and R. Felix, *Medchemcomm*, 2019, **10**, 1755–1764.
- 47 A. Mullard, *Nat. Rev. Drug Discov.*, 2021, **20**, 247–250.
- 48 L. M. Gockel, V. Pfeifer, F. Baltés, R. D. Bachmaier, K. G. Wagner, G. Bendas, M. Gütschow, I. Sosič and C. Steinebach, *Arch. Pharm. (Weinheim)*, , DOI:10.1002/ardp.202100467.
- 49 T.-T.-L. Nguyen, J. W. Kim, H.-I. Choi, H.-J. Maeng and T.-S. Koo, *Molecules*, 2022, **27**, 1977.
- 50
- 51 M. N. O'Brien Laramy, S. Luthra, M. F. Brown and D. W. Bartlett, *Nat. Rev. Drug Discov.*, 2023, **22**, 410–427.
- 52 C. Zhao and F. J. Dekker, *ACS Pharmacol. Transl. Sci.*, 2022, **5**, 710–723.
- 53 L. Zhang, B. Riley-Gillis, P. Vijay and Y. Shen, *Mol. Cancer Ther.*, 2019, **18**, 1302–1311.
- 54 S. B. Alabi and C. M. Crews, *J. Biol. Chem.*, 2021, **296**, 100647.
- 55 M. Rishfi, S. Krols, F. Martens, S.-L. L. Bekaert, E. Sanders, A. Eggermont, F. De Vloed, J. R. Goulding, M. Risseeuw, J. Molenaar, B. De Wilde, S. Van Calenbergh and K. Durinck, *Eur. J. Med. Chem.*, 2023, **247**, 115033.
- 56 A. F. Abdel-Magid, K. G. Carson, B. D. Harris, C. A. Maryanoff and R. D. Shah, *J. Org. Chem.*, 1996, **61**, 3849–3862.
- 57 S. E. Lazerwith, G. Bahador, E. Canales, G. Cheng, L. Chong, M. O. Clarke, E. Doerffler, E. J. Eisenberg, J. Hayes, B. Lu, Q. Liu, M. Matles, M. Mertzman, M. L. Mitchell, P. Morganelli, B. P. Murray, M. Robinson, R. G. Strickley, M. Tessler, N. Tirunagari, J. Wang, Y. Wang, J. R. Zhang, X. Zheng, W. Zhong and W. J. Watkins, *ACS Med. Chem. Lett.*, 2011, **2**, 715–719.
- 58 M. P. Schwalm, A. Krämer, A. Dölle, J. Weckesser, X. Yu, J. Jin, K. Saxena and S. Knapp, *Cell Chem. Biol.*, 2023, **30**, 753-765.e8.
- 59 B. Adhikari, J. Bozilovic, M. Diebold, J. D. Schwarz, J. Hofstetter, M. Schröder, M. Wanior, A. Narain, M. Vogt, N. Dudvarski Stankovic, A. Baluapuri, L. Schönemann, L. Eing, P. Bhandare, B. Kuster, A. Schlosser, S. Heinzlmeir, C. Sotriffer, S. Knapp and E. Wolf, *Nat. Chem. Biol.*, 2020, **16**, 1179–1188.
- 60 G. Proietti, K. J. Prathap, X. Ye, R. T. Olsson and P. Dinér, *Synth.*, 2022, **54**, 133–146.

61

- 62 M. R. Bauer, R. N. Jones, R. K. Tareque, B. Springett and A. Felix, 2019, **11**, 2491–2504.
- 63 Figures created and adapted using BioRender.com
- 64 Swiss Institute of Bioinformatics, Swiss ADME, <http://www.swissadme.ch/index.php>, accessed 04/09/23.